STScI | SPACE TELESCOPE SCIENCE INSTITUTE

Instrument Science Report STIS 2018-04

Monitoring the STIS Wavelength Calibration: MAMA and CCD First-Order Modes

Daniel E. Welty

August 30, 2018

Abstract

We discuss a uniform analysis of the wavelength calibration of STIS Pt/Cr-Ne lamp spectra that have been obtained for monitoring the accuracy of that calibration during cycles 7–11 and 17–25, focusing on the first-order MAMA and CCD settings. We have made improvements to the procedures that were used for previous analyses of some of those spectra, and have added accurate wavelengths for many Ne and Cr lines (from recent references) to the list of laboratory values used for comparison. We find that both the mean wavelength offsets and the scatter in the individual wavelength residuals have remained within the desired accuracies (0.2–0.3 pix, 1σ) for all of the first-order settings that have been monitored – though there has been some reduction in the number and strength of the lines measurable for some of the settings, due to the fading of the calibration lamps. As has been found in several previous studies, there are slight systematic trends (versus wavelength) in the wavelength residuals for some settings. We also note an apparent slight ($\sim$ 0.1 pix) shift in the mean offsets for most of the CCD settings that followed a change in the lamp used for the calibration observations in cycle 11. Additional changes have been made to the calibration observations in cycles 24 and 25 to compensate for the fading of the calibration lamps. We recommend that a re-calibration of the wavelengths be performed for the final archive of STIS observations, in order to correct the observed systematic deviations in the current calibration.

Contents

1. Introduction

The assignment of an accurate wavelength scale to each STIS spectrum is an essential aspect of converting raw STIS spectroscopic data into scientifically useful spectra. The STIS wavelength calibration was initially established by comparing pre-launch and early in-flight observations of the onboard Pt/Cr-Ne lamps with lists of rest wavelengths determined from laboratory studies, then fitting the measured positions of identified lines on the MAMA and CCD detectors to a simple, approximate model for the dispersion relations (Smith 1990; Hulbert et al. 1997; see also Espey 1999; Kerber et al. 2006a). The dispersion coefficients obtained in those early calibration programs have been applied to all subsequent STIS observations, with short contemporaneous lamp observations used to determine the zero point offset (e.g., due to slight differences in the position of the mode select mechanism) for each particular STIS spectrum (e.g., Baum 1997; Hulbert et al. 1997; McGrath et al. 1999; see also Lindler 1999). The continuing applicability and accuracy of that approach to the wavelength calibration of STIS spectra has been monitored on a roughly annual basis by obtaining sets of deeper spectra than those used for the offset determinations, for selected "representative" settings spanning the wavelength coverage of each of the available STIS gratings. The wavelengths measured for the lamp lines detected in those dispersion monitor spectra (assuming the default wavelength calibration) are compared with the corresponding laboratory values, in order to determine whether the wavelength calibration is within the desired absolute and relative accuracies [both typically of order 0.2-0.3 pix (1σ)].

While brief summaries of the results from the STIS dispersion monitor programs generally have been given in the annual STIS calibration close-out reports (see the list at the end of the References), a number of studies have examined the accuracies achieved in restricted subsets of the dispersion monitor spectra in more detail. Examples include analyses of CCD spectra from cycles 11 and 12 at pseudo-aperture E1 (Friedman 2005), selected MAMA echelle spectra from cycles 7–11 (Ayres 2008), a somewhat larger set of echelle spectra (Ayres 2010b), all of the CCD and MAMA spectra from cycle 17 (Pascucci et al. 2011; hereafter Pas11), and all of the CCD and MAMA spectra from cycles 19–21 (Sonnentrucker 2015; hereafter Son15). While all of those studies have indicated that the STIS wavelength

Table 1: STIS wavelength calibration monitoring programs

	MAMA programs			CCD programs			
Cycle	PID	Date	Lamp[a]	PID	Date	Lamp[a]	Comments
7	7078	1997jul	L/H1				image quality
	7722	1997aug	L/H1/H2	7722	1997aug	L/H1/H2	3.8, 10 mA for 3 lamps
	7649	1997dec	L	7648	1997sep	L	some echelle, a few G230B
	7651a	1998feb	L	**7650a**	1998mar	L	
	7651b	1999jan	L	**7650b**	1999jan	L	
8	**8430a**	1999aug	L	**8413a**	1999aug	L	
	8430b	2000aug	L	**8413b**	2000aug	L	
9				8850	2000jul	L	deep G750M
	8859	2000jul	L	**8848**	2000sep	L	
10	**8917**	2001aug	L	**8909**	2001aug	L	
11	**9618**	2002jun	L	**9617**	2002jun	H1	expanded sample
12	10031	2003dec	L	10025	2003sep	H1	a few deep exposures
				10087	2003dec	H2	GxxxL, a few G750M
17	11391	2009jul	L	11385	2009jun	H1	format verification
	11392	2009aug	L				format verification
	11859	2009aug	L	**11858**	2009aug	L/H1	expanded sample
	12079	2010apr	L/H1/H2	12079	2010apr	L/H1/H2	lamp comparisons
	12280	2010dec	L/H2				deep MAMA echelle (Ayres)
18	**12412**	2010nov	L	**12407**	2010nov	H1	
19	**12773**	2011oct	L	**12768**	2011oct	H1	
20	**13143**	2012oct	L	**13137**	2012oct	H1	
21	**13546**	2013oct	L	**13540**	2013oct	H1	
22	**13992**	2014nov	L	**13987**	2014nov	H1	
23	**14427**	2015nov	L	**14419**	2015nov	H1	
	14489	2016mar	H2				test HITM2 lamp
24	**14831**	2017may	L	**14825**	2017apr	H1	slight changes
25	**15391**	2018feb	L/H2	**15390**	2018mar	H1	slight changes

Notes: [a] L = LINE; H1 = HITM1; H2 = HITM2
Regular dispersion monitor programs are in bold type.

calibration has remained within the desired accuracies, slight systematic deviations in the wavelength residuals (the individual differences between observed and reference wavelengths), versus wavelength, have been noted for a number of the settings (e.g., Valenti 1996; Ayres 2008, 2010a, 2010b; Pas11; Son15).

In this report, we present the results of a uniform analysis of most of the first-order STIS spectra (using gratings G140L, G140M, G230L, G230M, G230LB, G230MB, G430L, G430M, G750L, G750M) obtained under the various dispersion monitor programs (and some other calibration programs) executed during cycles 7–11 and 17–25 (Table 1). Application of a uniform analysis procedure over a long baseline enables both a better assessment of the validity of that procedure and more reliable recognition and characterization of any subtle, but persistent systematic wavelength-dependent trends and/or temporal variations in the wavelength calibration. A subsequent report will cover the corresponding NUV-MAMA and FUV-MAMA echelle spectra obtained under those programs.

Table 2: Regularly monitored settings

Grating	λ range	$\Delta\lambda$ (Å/pix)	Cycles 7–11	Cycles 17–25
G140L	1150 – 1730	0.60	1425	1425
G140M	1145 – 1741	0.05	1218,1272,1420,1567,1714	1218,1640
G230L	1570 – 3180	1.58	2376	2376
G230M	1642 – 3099	0.09	1687,1933,2176,2419,2659,2898,3055	1687,3055
G230LB	1680 – 3060	1.35	2375	2375
G230MB	1635 – 3193	0.15	1713,1995,2416,2697,3115	1713[a],1995,2416,2697,3115
G430L	2900 – 5700	2.73	4300	4300
G430M	3022 – 5614	0.28	3165,3680,4194,4961,5471	3165,3680,4961,5471
G750L	5236 – 10266	4.92	7751,8975	7751
G750M	5448 – 10649	0.56	5734,6581,6768,8311,8561,9336,10363	5734,6768,8311,9336

Notes: [a] The G230MB/1713 setting was dropped in cycle 25 (too few measurable lines)

2. Monitoring Procedures

The task of monitoring the accuracy of the STIS wavelength calibration is complicated by several factors: the sheer number of modes and wavelength settings available for that versatile instrument, the availability of three different lamps for calibration (LINE, HITM1, HITM2 – which may be operated at currents of 3.8 or 10 mA), the somewhat unexpected wavelength-dependent fading of those three lamps with time (e.g., Pascucci et al. 2010a, 2010b, 2010c; Peeples 2017; see also Kerber et al. 2006b; Nave et al. 2008, 2012), and the temporal changes in the sensitivity of the MAMA and CCD detectors (e.g., Carlberg & Monroe 2017). In practice, "representative" settings spanning the wavelength coverage of each of the first-order and echelle gratings have been selected for annual monitoring – though there have been some changes in the selections over the years (e.g., for cycles 7–11 versus for cycles 17–25); Table 2 lists the most regularly observed settings for those two periods. Additional settings were included in the annual monitoring programs in cycles 11 and 17, and some special calibration programs (e.g., comparing the spectra from different lamps, taking deeper spectra of some settings) were executed in individual cycles; see Table 1.

As noted in Table 1, most of the programs for the MAMA have employed the LINE lamp for most (if not all) settings, while the programs for the CCD switched from the LINE lamp to the HITM1 lamp after cycle 10. While all three of the onboard Pt/Cr-Ne lamps are fading, the decline in emission line strengths is particularly pronounced for the LINE lamp at wavelengths below about 1350 Å (e.g., Pascucci et al. 2010c; Peeples 2017). Several of the shortest wavelength settings therefore have recently been switched to the HITM2 lamp (which now has stronger lines than the LINE lamp below about 1270 Å), in order to enable detection and measurement of sufficient sets of lines at those short wavelengths. For some other settings, the lamp current has been increased from the original 3.8 mA to 10 mA – which yields both a general increase in the strengths of the emission lines and differences in the relative strengths of lines from different species (e.g., Kerber et al. 2004, 2006b).

The analysis of the dispersion monitor data begins by treating the lamp spectra as science exposures. A python script is used to change header keywords and flags, to process the raw 2-D data through the **calstis** pipeline, and to extract the 1-D spectra (using a 300 pixel extraction box centered on pixel 512). The wavelength scale is assigned via the standard

dispersion relations (with the zero point determined from the data themselves, rather than from a separate wavecal exposure). No background corrections, flux calibrations, or Doppler corrections are performed. In most cases, only single exposures were obtained for the CCD settings, so that no removal of cosmic rays is performed – which can be problematic for several of the shorter wavelength G230MB settings (with longer exposure times), due to the relatively large extraction box. As discussed in more detail below, a procedure coded in IDL is then used to measure the wavelengths of discernible emission lines and to compare those measured values with a list of laboratory wavelengths, in order to determine – for each setting at each epoch – the mean offset between the measured and fiducial wavelengths, the scatter in the residuals, and any systematic trends in the residuals. Those characteristics are then compared between different cycles, to see if there are any significant temporal trends in the accuracy of the wavelength calibration.

2.1. Line Lists

Because the various available STIS modes cover a large range in wavelength (from about 1150 to 10650 Å), Pt/Cr-Ne hollow cathode lamps were chosen for the wavelength calibration – with Pt providing the majority of the lines below 3200 Å, Ne most of the lines above 5400 Å, and Cr most of the lines in between. The lists of laboratory wavelengths used for the initial STIS wavelength calibrations were compiled by D. Lindler from several sources: the measurements of lines in Pt-Ne lamp spectra performed by Reader et al. (1990), the wavelength tables maintained at NIST, and other references. Custom subsets of those lines were used to calibrate the various STIS modes – e.g., excluding lines that would be blended in the lowest-resolution GxxxL-mode spectra. Those initial line lists were later augmented and refined via new laboratory measurements of the lines in Pt/Cr-Ne lamp spectra (Sansonetti et al. 2004) and via slight empirical adjustments based on measurements of the lines in deep STIS echelle wavelength calibration spectra (Ayres 2010b) – but only between about 1130 and 3150 Å. The analyses of post-SM4 STIS wavelength calibration spectra reported by Pas11 and Son15 used several of those wavelength lists: primarily Sansonetti et al. (2004) and Ayres (2010b) for the shorter wavelength settings (G140, E140, G230, E230, G230B) and values obtained from NIST and from a list of longer wavelength lines provided by D.

Table 3: Wavelength compilations: mean wavelength differences vs. current NIST values

Reference	Coverage		$\Delta\lambda$(Cr)		$\Delta\lambda$(Ne)		$\Delta\lambda$(Pt)	
	(Å)	N	(mÅ)	N	(mÅ)	N	(mÅ)	N
Reader et al. 1990 (PtNe)	1100 – 4000	>3000	NA	...	...	...	...	...
initial STIS (Lindler; PtCrNe)	1164 – 10613	2390	-1.92 ± 0.96	110	0.97 ± 0.12	441	-5.79 ± 0.88	146
LindPC (Lindler; PtCrNe)	2914 – 9967	798	7.13 ± 0.92	386	0.56 ± 0.39	351	0.29 ± 0.02	36
Sansonetti et al. 2004 (PtCrNe)	1131 – 1828	1232	0.53 ± 0.74	199	0.52 ± 0.01	71	...	5
Kramida & Nave 2006a (Ne III)	204 – 360000		NA	...	...	...	NA	...
Kramida & Nave 2006b (Ne II)	324 – 130000	>1700	NA	...	...	...	NA	...
Wallace & Hinkle 2009 (Cr I)	2366 – 54287	1975	0.00 ± 0.00	1532	NA	...	NA	...
Ayres 2010b (PtCrNe)	1151 – 3150	5698	-0.07 ± 0.31	1688	0.36 ± 0.04	356	-6.03 ± 1.21	147
NIST (Pas11/Son15; PtCrNe)	1131 – 4333	5627	...	7	-0.55 ± 0.17	695	-7.02 ± 0.90	185
Sansonetti et al. 2012 (Cr II)	1142 – 3954	3604	-0.02 ± 0.01	3367	NA	...	NA	...
Sansonetti & Nave 2014 (Cr II)	2850 – 37857	5362	0.02 ± 0.00	4758	NA	...	NA	...
this study (all; PtCrNe)	1131 – 54287	14252	...	...	...	...	...	...
this study (G430, G750; PtCrNe)	1131 – 45917	6430	0.08 ± 0.15	993	0.32 ± 0.16	1281	-6.69 ± 0.86	193

Lindler (a revised version of the list used for the original calibrations; hereafter referred to as "LindPC") for the longer wavelength settings (G430, G750)[1]. More recent measurements of the lines produced by Cr-Ne, Cr-Ar, and Fe-Ne hollow cathode lamps, however, have increased the samples of accurate wavelengths for Cr I and Cr II (Wallace & Hinkle 2009; Sansonetti et al. 2012; Sansonetti & Nave 2014) and for Ne I, Ne II, and Ne III (Kramida & Nave 2006a, 2006b), particularly at longer wavelengths. While the newer values for Cr and Ne have now been incorporated into the line lists maintained at NIST, the current NIST list for Pt needs updating (e.g., it does not include the values from Sansonetti et al. 2004). Table 3 lists the various wavelength compilations used in previous studies of the STIS wavelength calibration and/or incorporated in this study, with information on the wavelength range covered, the number of lines included, and the mean wavelength differences (separately for Cr, Ne, and Pt) relative to the values currently available at NIST.

We have compared the wavelengths and line intensities listed in the various references given in Table 3 – first to determine how well the values agree for lines in common and then to assemble a new merged list of lines, on a common wavelength and intensity scale (as much as possible), for comparison with the STIS wavelength calibration spectra. Below about 4330 Å, the agreement in wavelength is generally reasonably good (within several mÅ) for the lines in Sansonetti et al. (2004), the NIST list used by Pas11 and Son15, and the list described by Ayres (2010b) – both among those three lists and versus the current NIST values (for Cr and Ne). The overall mean wavelength differences for each reference (for each element, relative to the current NIST values), listed in the last six columns of Table 3, are generally less than 1 mÅ for Cr and Ne, but are larger for Pt (where the NIST values need updating). There is much greater scatter (differences of tens of mÅ), however, for a number of the longer wavelength Cr and Ne lines in the LindPC list, compared to the more recent values now incorporated into the NIST compilations (Appendix Figure 7). While even the largest of those differences correspond to a small fraction of a pixel for the G750L settings, a difference of 100 mÅ corresponds to nearly 0.2 pixel for the G750M settings. As the LindPC list is very similar to the list used in the original wavelength calibration, and as it apparently was the only list used by Pas11 and Son15 that includes lines beyond about 4330 Å, those differences between the older and current reference wavelengths suggest that some revisions to the wavelength calibration (and its evaluation) might be in order. Comparisons of the line strengths among the various line lists are more difficult, however, as different lamps, operating under different conditions, were used in the corresponding laboratory studies. We have attempted to bring the intensities to a (roughly) common scale (that of the older NIST list used by Pas11 and Son15) by multiplying the values for each species and reference by a constant determined from lines in common with that older NIST list – but those constant scaling factors are not well defined or determined in some cases.

Our final merged list includes more than 14000 lines, ranging from 1131 Å to 5.43 μm (Table 3). For comparisons with the shorter wavelength spectra from G140, G230, and G230B, we have adopted the Ayres (2010b) wavelengths (slightly augmented to extend the coverage to 3200 Å). For comparisons with the longer wavelength spectra from G430 and

[1]While both Pas11 and Son15 also cite Wallace & Hinkle (2009), only the lines below 3150 Å were included (through the Ayres 2010b compilation); the many Cr I lines at longer wavelengths from that source were not included.

G750, we have adopted the Cr and Ne wavelengths currently in NIST (based on the recent studies noted above; but omitting the weaker lines that are generally not detected in the STIS spectra), plus the Pt wavelengths from the older NIST and LindPC lists.

2.2. Line Identification and Fitting

The initial analyses of the extracted 1-D wavelength calibration spectra utilized the legacy IDL code that had been employed by Pas11 and Son15 in their analyses of the spectra from cycles 17–21. For each first-order setting, that code marches through the spectrum, looking for measurable emission features within 0.5 pixel of the expected positions of lines in the fiducial lists. For each recognized emission feature, the line center is estimated in three ways: as the wavelength of peak intensity, via an intensity-weighted average of the wavelengths of the five points nearest the peak, and via a Gaussian fit to the overall line profile.[2] Features that are deemed too narrow (e.g., due to cosmic rays) or too broad (e.g., due to blends of two or more lines) are rejected – with different cut-off widths for the different gratings and modes; Son15 also removed obviously blended or saturated lines. The values for the centroids of the remaining "valid" matches are saved in a log file, and the mean wavelength offset (relative to the laboratory values) and standard deviation of the residuals are computed for each method.

After examination of the results of those initial analyses, some changes were made to the code and procedure – to fix several problems that were identified, to incorporate additional capabilities, and to reduce the need for user intervention:

- In the legacy code, a number of the lines longward of 2000 Å in the NIST list were not converted from air to vacuum values (which is necessary for comparisons with the STIS spectra), and some of the LindPC lines were not included in the combined reference list. That, together with the incompleteness of the previously available lists for Cr and Ne beyond about 3150 Å, meant that a number of lines that are consistently detectable in the spectra were either misidentified or not identified in a number of the settings (especially G430L/4300 and G430M/3165-4194). Performing the appropriate air-to-vacuum conversions and incorporating additional Cr and Ne lines from more recent references significantly increased the number of lines (N) correctly identified in those settings (Appendix Table 12; note that the N values for this study do not include lines considered to be blended).

- In the legacy code, matching of the observed emission features with lines in the reference lists did not take into account the relative strengths of the reference lines; in all cases, the closest match in wavelength (within 0.5 pixel) was adopted. For some settings, however, the density of lines in the combined reference lists is high enough that some observed emission features were matched with weak lines that happened to be slightly closer in wavelength, instead of the stronger (but slightly more distant) lines that should have been assigned. Such mismatches would presumably have yielded

[2] As Gaussians generally gave good fits to the profiles (except for some saturated, asymmetric lines in several of the longer wavelength G140M and G230M settings) – and as the Gaussian fits also provide convenient measures of line strength – we have adopted the Gaussian fits in this study.

smaller mean wavelength offsets and smaller scatter in the residuals than would have been obtained for the correct matches. The match criterion was therefore changed to associate each detected emission feature with the strongest line in the reference lists within 0.5 pixel (instead of the nearest line). While that criterion yields reasonable matches in most cases, the difficulty of assigning accurate relative strengths to lines from different species (in the reference lists) does lead to some ambiguity for a small number of lines.

- Not all of the emission features due to cosmic rays (especially in the longer CCD exposures) or due to blends of several lamp lines were eliminated by the line width restrictions. While some weak lamp lines could be reliably measured in early G230MB/1713 spectra, for example, cycle-to-cycle inconsistencies in the set of lines found in the post-SM4 spectra suggest that the lamp had faded enough that most of the lines "identified" in those more recent spectra are actually due to cosmic rays. On the other hand, some blended features dominated by a single relatively strong line are not broad enough to be rejected as obvious blends, but their centroids can still be affected by the weaker lines contributing to the blends. Such features are now flagged if the potential contributions from weaker lines to the total (blended) line strength exceeds 10%. For each setting, separate statistics are now calculated for all the detected lines, for the subset of unblended lines, and for the subset of lines consistently detected (cycle to cycle) in the spectra. The lines that are both unblended and consistently detected should give the most reliable measure of the mean offset and scatter in each setting.

- A measure of the strength of each detected line – the product of the height and width of the fitted Gaussian – is now computed and saved in the log file. Those data enable quantitative tracking of the temporal changes in line strength – due to the combination of changes in the detector sensitivity (e.g., Carlberg & Monroe 2017) and the fading of the calibration lamps (e.g., Peebles 2017) – as functions of wavelength and (in principle) species within each setting. They have also informed decisions regarding changes to the monitoring observations themselves – e.g., eliminating a setting for which too few lines are now measurable, increasing the lamp current or switching lamps for a given setting to yield more measurable lines.

A single master copy of the IDL code for each grating (which incorporates the various corrections and enhancements noted above) is now used to analyze the available dispersion monitor data from all cycles, so that any further modifications of the procedure can be quickly and uniformly applied to all the data. Additional IDL procedures have been developed to compare both the spectra and the results of the analysis from different cycles.

As an example, Figure 1 shows the results of the line-fitting procedure for the G430M/3680 spectrum (and the corresponding part of the lower-resolution G430L/4300 spectrum) from cycle 17. While most of the lines in the G430M spectrum appear to be correctly identified and fitted, several of the lines in the G430L spectrum (near 3665 and 3778 Å) are misidentified. Both the density of lines in the reference list (compared to the resolution of the G430L spectrum) and the evident differences between the relative line strengths given in the reference list and those actually observed are likely to have contributed to those misidentifications. There is also at least one line in the G430L spectrum (near 3714 Å) for which

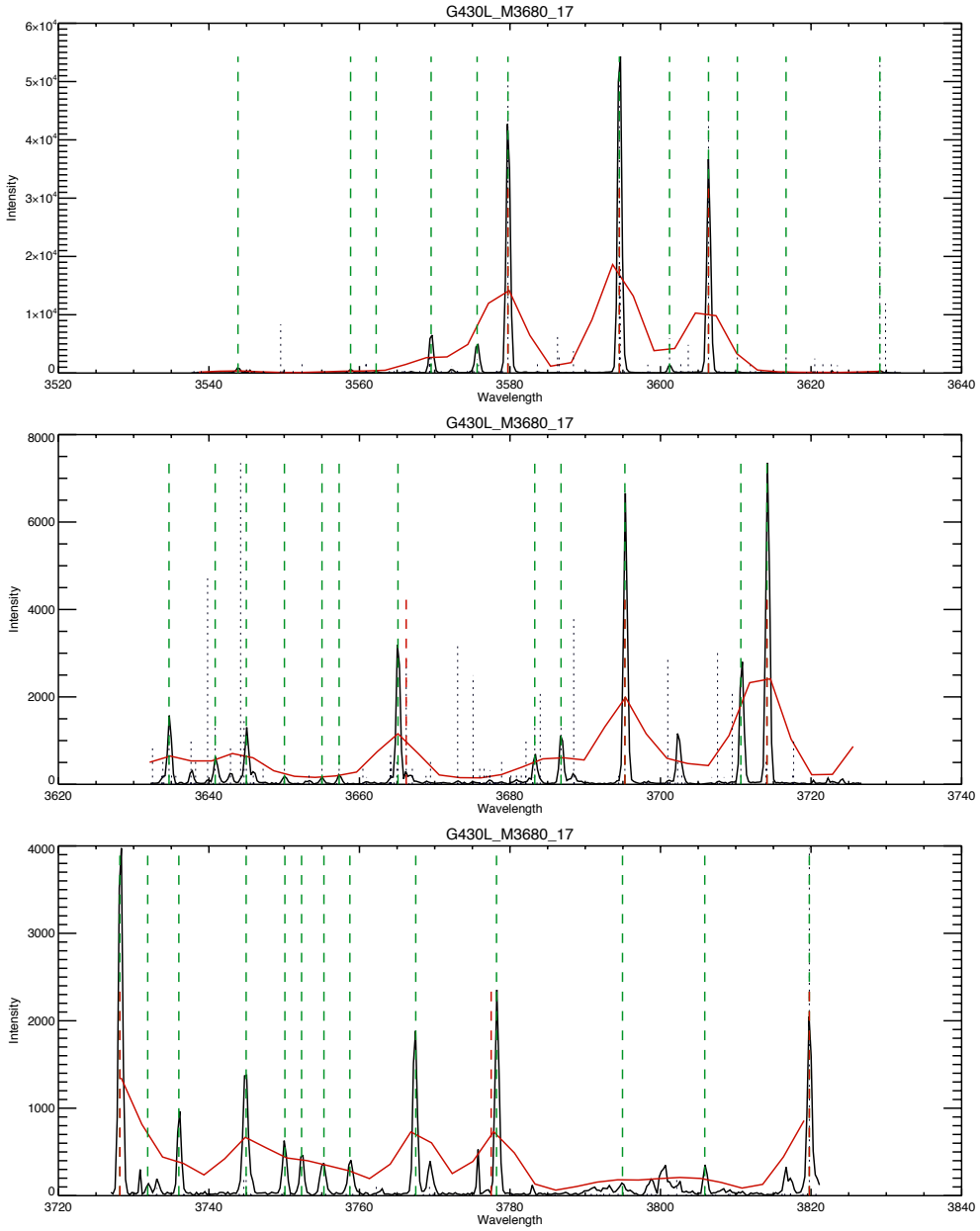

Figure 1: Spectra from cycle 17 of G430M/3680 (black) and G430L/1425 (red). Lines from the reference lists are given by dotted black lines (with height proportional to the listed strength); detected / measured lines are given by dashed green (G430M) and red (G430L) lines (at the laboratory wavelengths). One pixel corresponds to 0.28 Å for G430M and to 2.73 Å for G430L. Note the differences in vertical scale among the three panels, the effects of line density / blending (especially for the G430L spectrum), and the differences between the relative line strengths in the reference list versus in the observed spectrum.

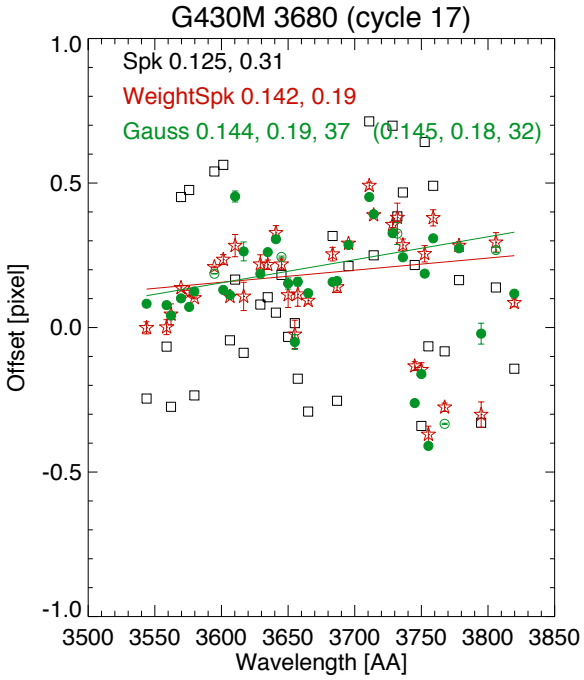

Figure 2: Wavelength residuals (in pixels) for the G430M/3680 setting (cycle 17) shown in Fig. 1. Black squares are for the peak wavelengths; red stars are for the weighted averages; green circles are for the Gaussian fits (open circles are for blended features). The mean offsets, standard deviation of the residuals, and (for the Gaussian fits) the number of points are given at the top; the values in parentheses for the Gaussian fits are for the unblended lines. The red and green solid lines are linear fits to the weighted fit and Gaussian fit points, respectively.

blending has shifted the centroid of the line away from the position of the dominant contributor to that blended feature. For the 32 unblended lines measured in the G430M/3680 spectrum, the mean offset (for wavelengths obtained from the Gaussian fits, relative to the reference wavelengths) is 0.15 pix, and the standard deviation of the residuals is 0.18 pix (Fig. 2; Appendix Tables 6, 8, and 11). Linear fits to the residuals (for both the weighted and Gaussian fits) suggest no significant trends with wavelength for this setting; there are several apparently "discrepant" points, however (e.g., near 3750 Å). Only 6–8 lines could be measured in the corresponding part of the G430L/4300 spectrum, due to blending issues.

3. Results

The main results of the analysis of the dispersion monitor spectra from cycles 7–11 and 17–25 are given compactly in Figures 3, 4, and 5, which show the mean wavelength offsets (for the Gaussian fits), the standard deviations of the residuals, and the mean relative line strengths, respectively, for the unblended lamp lines measured for each of the regularly monitored settings of the five first-order gratings, as functions of time. In each panel of those figures, the black lines give the values for the L-mode spectra noted in the title to the panel, while the colored lines give the values for the corresponding higher-resolution M-mode spectra noted in the middle of the panel. Table 4 lists the average values (for cycles 7–11 and 17–25) of the mean offsets, the standard deviations of the residuals, and the number of consistently detected unblended lines for each regularly monitored setting. The average values presented in Figures 3–5 and in Table 4 are based primarily on the detailed cycle-by-

cycle lists of those quantities contained in Appendix Tables 5–11. The average residuals for the individual lines measured in each setting in cycles 7–11 are shown (versus wavelength) in Appendix Figures 8–12. In those figures, lines measured in at least one cycle (all) are given by "+", unblended lines (nob – for no blend) are given by open squares, and lines measured in at least five of the seven data sets (5–7) are given by "x"; the most reliable lines (gnb – for good, no blend) are thus given by a superposition of all three symbols.

Mean offsets: With one notable exception, the mean wavelength offsets (for wavelengths obtained from the Gaussian fits) exhibit roughly constant, but often apparently non-zero values for each monitored setting (Fig. 3; columns 4 and 10 of Table 4; see also Appendix Tables 5 and 6). The exception is the apparent ∼0.1 pix increase in the mean offsets for most of the CCD settings when the lamp was switched from LINE to HITM1 in cycle 11 (Table 4, last column). (Note that the mean offsets for the post-SM4 cycles 17–25 are consistent with those for cycle 11, for those CCD settings, and are generally higher than the values for cycles 7–10.) As noted by Pas11, the wavelength calibration appears not to have changed significantly during the period between cycles 12 and 17 (when STIS was not operational). The absolute values of the mean offsets are in all cases less than 0.3 pix, and in most cases are less than 0.2 pix. For example, the mean offsets for the different settings range from 0.00 to 0.13 (G140), -0.26 to 0.03 (G230), -0.03 to 0.05 (G230B), -0.19 to 0.05 (G430), and -0.19 to 0.05 (G750) for cycles 7–11, and from -0.03 to 0.23 (G140), -0.24 to 0.07 (G230), 0.00 to 0.21 (G230B), -0.11 to 0.15 (G430), and -0.08 to 0.08 (G750) for cycles 17–25. At least some of the cycle-to-cycle differences and possible weak secular trends seen for some settings in Figure 3 (e.g., the possible slight increases for G230LB, G430L, and G750L over cycles 17–25) appear to be due to differences in the set of lines detected and successfully measured in each case (e.g., as the calibration lamps fade).

Cross-correlation of spectra for a given setting but from different cycles – which should be less sensitive to differences in the sets of detected lines – generally yielded similar relative mean offsets to those determined from fitting individual lines. That method does not reveal possible trends in the residuals with wavelength within a given setting, however, and is less straightforward for comparing spectra at the position of the E1 pseudo-aperture with those taken at the nominal (central) position, due to slight changes in the dispersion with y-position on the detector.

Residuals / scatter: In general, the standard deviations of the wavelength residuals are smaller for the subset of unblended, consistently detected lines, compared to the values for the full set of measured lines (columns 6 and 12 versus columns 5 and 11, respectively, in Table 4). For most of the settings, the standard deviations for the unblended lines appear to have remained roughly constant, with average values less than 0.25 pix (Fig. 4; columns 6 and 12 of Table 4; see also Appendix Tables 7 and 8) – though the post-SM4 selection of settings is somewhat different and the number of lines consistently detected (for settings in common) has decreased, in many cases. For example, the mean standard deviations for the different settings range from 0.16 to 0.24 (G140), 0.18 to 0.24 (G230), 0.11 to 0.17 (G230B), 0.10 to 0.17 (G430), and 0.06 to 0.13 (G750) for cycles 7–11, and from 0.09 to 0.23 (G140), 0.14 to 0.20 (G230), 0.09 to 0.20 (G230B), 0.07 to 0.20 (G430), and 0.03 to 0.10 (G750) for cycles 17–25. Again, some of the cycle-to-cycle differences in the standard deviations for a given setting appear to be related to differences in the number of lines that were measured (e.g., for G140M/1640).

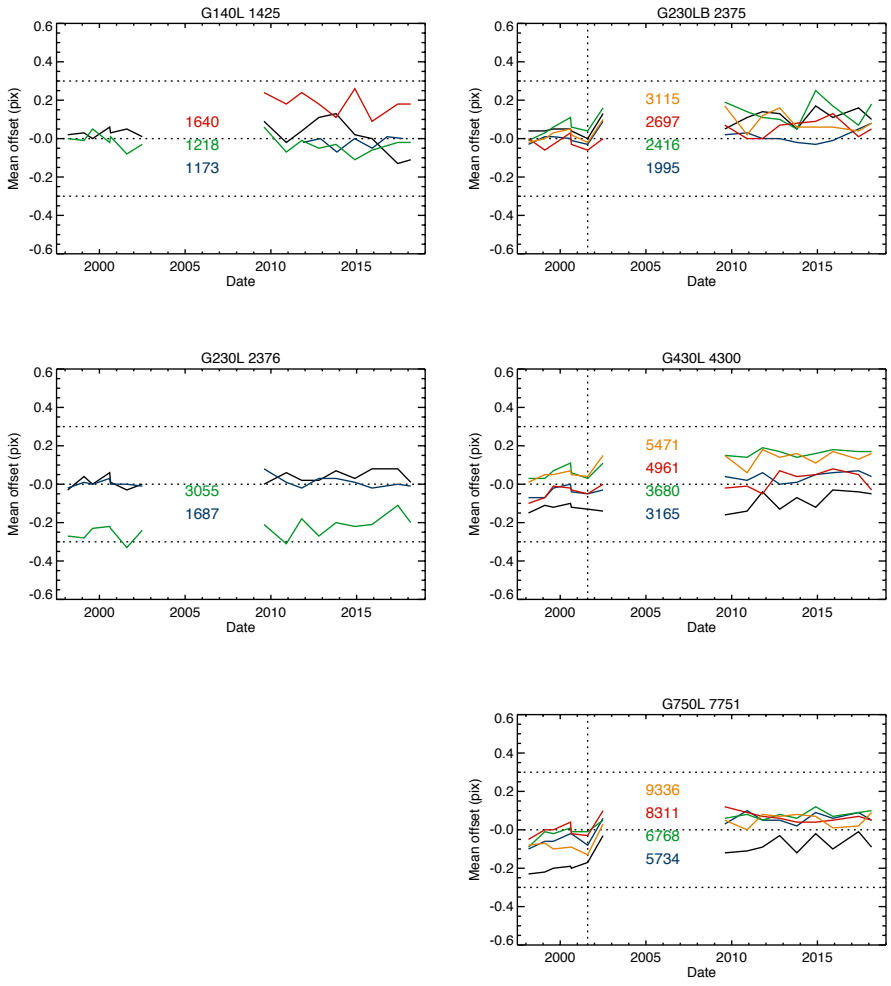

Figure 3: Mean wavelength offsets (in pixels) for unblended lines measured in regularly monitored settings. The left-hand panels are for the first-order MAMA settings; the right-hand panels are for the first-order CCD settings. In each panel, the black line is for the L-mode setting given in the title of the panel, while the colored lines are for the corresponding M-mode settings noted in the middle of the panel (where STIS was not operational). The vertical dotted lines for the CCD mark the last data obtained with the LINE lamp (cycle 10); subsequent cycles have used the HITM1 lamp. While the mean offsets for most settings have remained roughly constant (and within the desired accuracy of 0.2-0.3 pix), there appears to have been a slight ($\sim$ 0.1 pix) increase in the offsets for a number of the CCD settings after the switch to the HITM1 lamp.

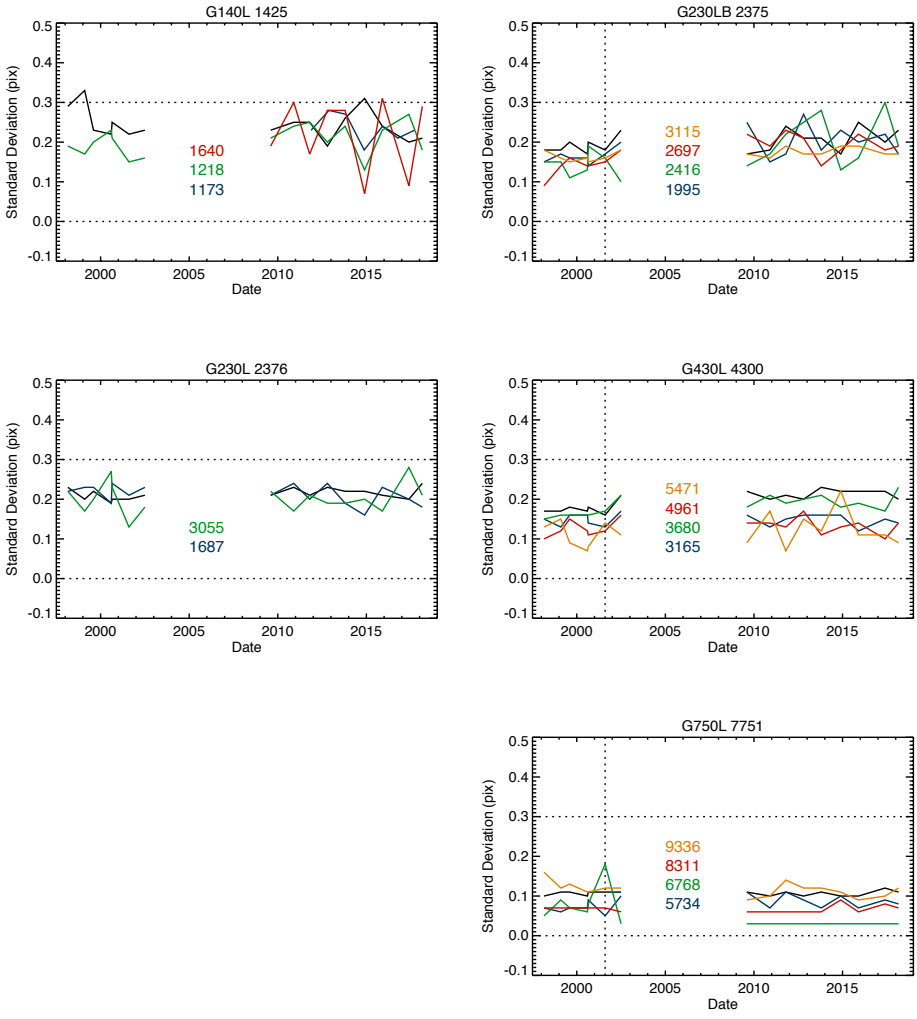

Figure 4: Standard deviations of wavelength residuals (in pixels) for unblended lines measured in regularly monitored settings. The left-hand panels are for the first-order MAMA settings; the right-hand panels are for the first-order CCD settings. In each panel, the black line is for the L-mode setting given in the title of the panel, while the colored lines are for the corresponding M-mode settings noted in the middle of the panel (where STIS was not operational). The vertical dotted lines for the CCD mark the last data obtained with the LINE lamp (cycle 10); subsequent cycles have used the HITM1 lamp. While the scatter may have increased slightly for some of the settings, the most recent values are all ≤ 0.3 pix.

Line strengths: The wavelength-dependent fading of the calibration lamps (e.g., Peeples 2017) has led to corresponding declines in both the strengths of the measured lines and the number of lines detected – particularly at the shorter wavelengths (Fig. 5 and Appendix Table 9; Appendix Tables 10 and 11). The decrease in the number of lines is most dramatic for the subset of unblended, consistently detected (gnb) lines, which constitute a smaller fraction of the total detected lines in cycles 17–25 (columns 8 and 14, relative to columns 7 and 13, in Table 4). In Figure 5, the average line strengths for each setting in cycles 7–11 are shown relative to the values found in the early part of cycle 7; for cycles 17–25, the normalization is to the values found in cycle 17 (except for G140M/1173, which is normalized to cycle 19). That dual normalization is most appropriate for the CCD data (as the lamp for all CCD settings was switched from LINE to HITM1 in cycle 11) and for the G140M/1173 data (as the lamp for that setting was switched from LINE to HITM2 in cycle 19). It is somewhat misleading, however, for the rest of the MAMA data – for which the lamp and (in most cases) lamp current have not changed (except for several of the settings in cycles 24 and 25).[3] Normalizing the strengths of the lines in the cycle 24 G140M/1218 spectrum by the corresponding values from cycle 7, for example, indicates that the strengths decreased by a factor of about 40 (on average), and by an even larger factor at the shortest wavelengths. These declines in line strength are consistent with the results of Peeples (2017) and with the trends seen in a compilation of data for all of the calibration lamps[4]– both of which are based on total count rates over the entire images. Figure 5 also indicates that the strengths of the lines in the MAMA/G230 settings are declining more rapidly than those of the corresponding lines in the CCD/G230B settings. Figure 6 shows the line strength ratios (cycle 23 vs. cycle 17) for the individual lines measured in each of the five L-mode spectra. For all except the G750L/7751 setting, the ratios appear to be systematically smaller at the shorter wavelength end of the setting; that trend is especially clear for G140L/1425 below about 1350 Å. The severe declines in line strength at the shortest wavelengths – which cannot be ascribed to changes in detector sensitivity (e.g., Carlberg & Monroe 2017) – motivated the switch to the HITM2 lamp (which is now brighter than the LINE lamp below about 1270 Å, and is fading less rapidly) for several MAMA settings in cycle 25.

Systematic trends: Several previous studies of the STIS wavelength calibration have found slight systematic trends in the wavelength residuals vs. wavelength for some MAMA E140 and E230 echelle settings (Valenti 1996; Ayres 2008, 2010a, 2010b; Pas11; Son15). Similar trends were difficult to discern in the first-order grating spectra in the latter two references, however, due largely to the relatively small number of lines identified and measured in many of the G140M, G230M, G230MB, G430M, and G750M settings. In the present study, the use of an expanded reference line list has enabled the identification of many more lines, particularly for some of the G230B and G430 settings (Appendix Table 12). Moreover, comparison of the results from many cycles indicates sets of lines that are both unblended and consistently detected. Averaging the observed residuals for those most reliably measured lines over several cycles then can provide a clearer view of any possible trends in the residuals.

[3]The current for G140L/1425 and G230M/3055 was changed from 3.8 to 10 mA in cycle 24 (producing both an overall increase in line strengths and changes in the relative strengths of lines from different species); the lamp for E140H/1271 and G140M/1218 was switched from LINE to HITM2 in cycle 25.

[4]available at http://www.stsci.edu/~STIS/monitors/lamp/stis_lamps.pdf

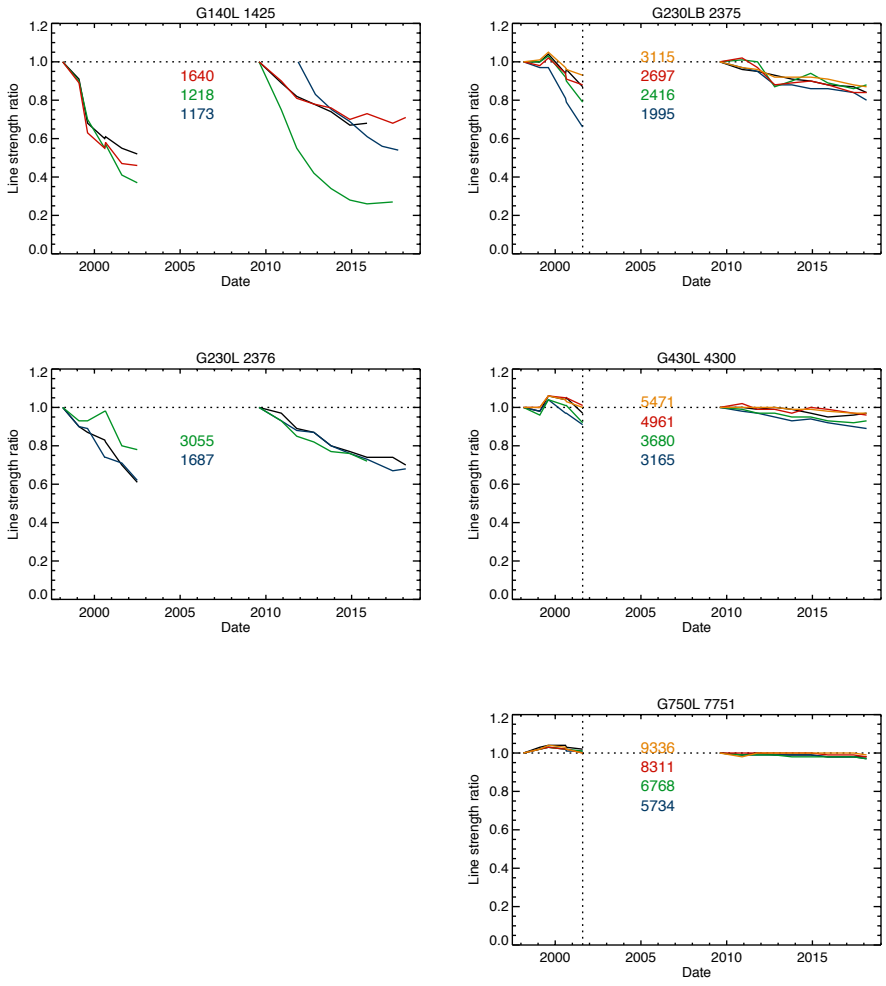

Figure 5: Mean ratios for strengths of lines measured in regularly monitored settings. The left-hand panels are for the first-order MAMA settings; the right-hand panels are for the first-order CCD settings. In each panel, the black line is for the L-mode setting given in the title of the panel, while the colored lines are for the corresponding M-mode settings noted in the middle of the panel (where STIS was not operational). The vertical dotted lines for the CCD mark the last data obtained with the LINE lamp (cycle 10); subsequent cycles have used the HITM1 lamp. The values for cycles 7–10 are normalized to the early cycle 7 strengths; the post-SM4 (cycle 17–25) values are normalized to the cycle 17 strengths. Note that the declines for the G230B (CCD) settings are less severe than for the corresponding G230 (MAMA) settings. At the shortest wavelengths, the strengths of lines in the LINE lamp spectra are now only several percent of their initial values in cycle 7; several of those settings have now been switched to HITM2 (which is now brighter below about 1270 Å).

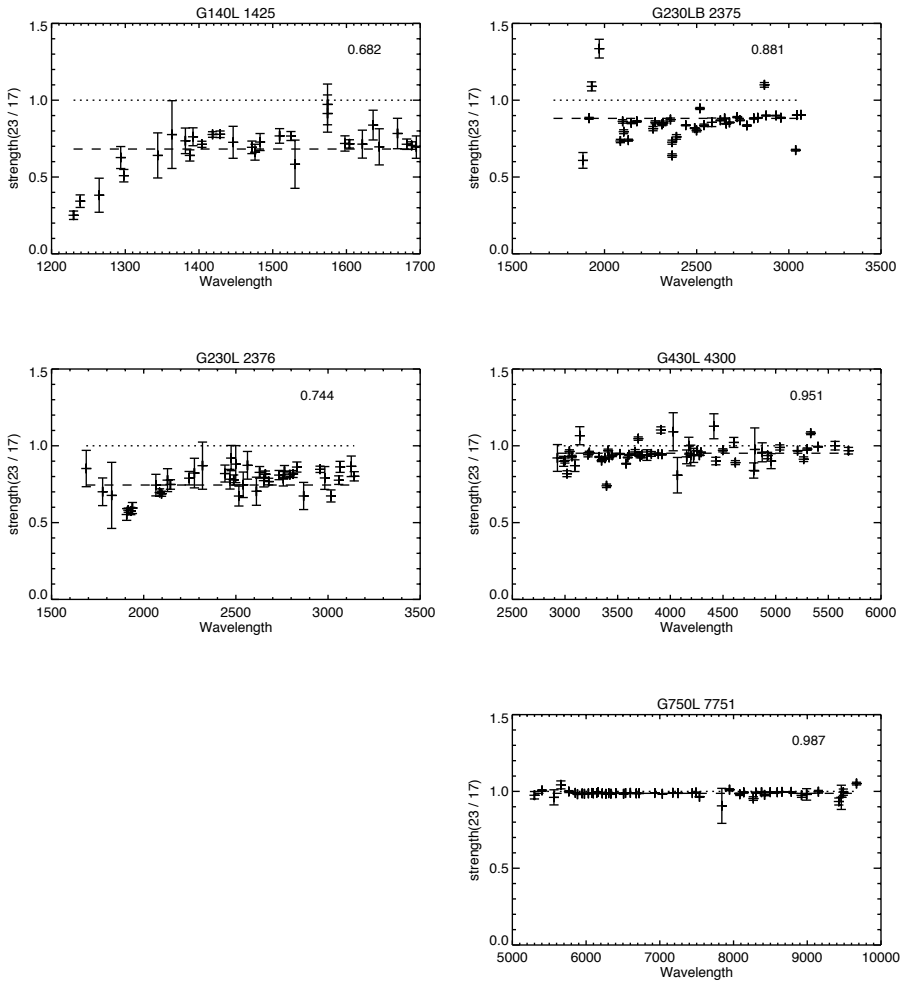

Figure 6: Line strength ratios (cycle 23 vs. cycle 17) for individual lines in all five L-mode settings. The weighted mean ratio (noted at upper right; with weights based on the uncertainties on the ratios for the individual lines) is given by the horizontal dashed line; there is a general tendency for the ratios to be smaller at the shorter wavelengths in each setting, however – especially for G140L/1425 below about 1350 Å.

Appendix Figures 8–12 show the average residuals for the individual lines measured for most of the first-order grating settings observed in cycles 7–11. As noted above, the most reliably measured lines (gnb) are those marked by a combination of the "+", "x", and open square symbols. While the number of points is still relatively small and/or the scatter is still fairly large for some settings, there do appear to be cases of consistently non-zero mean offsets (i.e., where the residuals for the gnb lines are predominantly positive or negative; e.g., G230M/2659, G230M/3055, G430M/4194, G750L/7751, G750L/8975; see also Fig. 3 and Table 4) and of possible linear or non-linear trends in the residuals with wavelength (e.g., G140M/1420, G140M/1714, G230L/2376, G230MB/1995, G230MB/2697, G230MB/3115, G430M/5471, G750M/8311, G750M/9336). A different set of CCD settings exhibits consistently non-zero mean offsets in the post-SM4 data, due to the apparent ∼0.1 pixel increase in mean offsets following the change in lamp after cycle 10 (Table 4). Some consistently "discrepant" points may also be noted in some of the settings. In principle, systematic deviations in the wavelength calibration near the ends of the wavelength coverage of a given setting can produce disagreements in the wavelengths in the regions of overlap with adjacent settings.

In several studies of the wavelength calibration of STIS echelle spectra, Ayres (2008, 2010a, 2010b) has argued that such systematic trends in the wavelength residuals are likely due to the combined effects of a too-simple parameterization of the dispersion relations, relatively small numbers of lines used for the original calibration of some settings, and/or persistent small-scale geometric distortions in the detectors (i.e., apart from the optical effects) – and that such trends can be significantly reduced by the incorporation of additional higher-order terms in the dispersion relations. The current STIS echelle dispersion relations are parameterized as

$$s = A_0 + A_1 m\lambda + A_2 (m\lambda)^2 + A_3 m + A_4 \lambda + A_5 m^2 \lambda + A_6 m\lambda^2$$

(e.g., Hulbert et al. 1997), where s is the position along the dispersion direction, m is the order number, and the $A_{\rm n}$ are the dispersion coefficients. For the first-order grating spectra ($m = 1$), that formula reduces to a quadratic in λ. For the echelle spectra, Ayres (2010b) found that the use of a more extensive set of accurate reference wavelengths and the addition of two terms [m^2 and $(m\lambda)^3$] to the dispersion relations yielded the most significant overall improvements to the echelle wavelength solutions.[5] Adding other higher-order terms to the dispersion relations for individual echelle settings further improved the results for those particular settings (Ayres 2010a). Analyses of the MAMA echelle mode spectra obtained in cycles 7–11 and 17–25 – and comparisons with the trends found by Ayres (2008, 2010a, 2010b), Pas11, and Son15 – will be explored in a subsequent report.

Changes: During the past two cycles (24 and 25), a number of changes were made to the dispersion monitor observing programs in order to compensate for the fading of the calibration lamps. In cycle 24, the operating current for the G140L/1425 and G230M/3055 settings was increased from 3.8 mA to 10 mA – yielding both general increases in the strengths of the

[5]Initial indications of increased residuals for some echelle settings following the incorporation of those terms were found to be due to the monthly offsets of MAMA spectra that were performed between 1998 January and 2002 August (i.e., for most of cycles 7–11; Pas11; see also Lindler 1999).

Table 4: Monitored settings: average values (first-order MAMA and CCD)

Grating	Wave	Cycles 7–11 Offset		StDev		Nlines		Cycles 17–25 Offset		StDev		Nlines		17–25 vs.
		all	good[a]	all	good[a]	all	good[a]	all	good[a]	all	good[a]	all	good[a]	7–11[b]
G140L	1425	−0.01	0.08	0.25	0.21	61	14	−0.04	0.00	0.23	0.17	73	11	−0.08
G140M	1173							−0.02	−0.02	0.23	0.23	11	11	
	1218	−0.05	0.00	0.22	0.16	29	20	−0.03	−0.03	0.22	0.19	28	9	−0.03
	1272	0.11	0.13	0.30	0.22	33	18							
	1420	0.03	0.02	0.26	0.20	43	28							
	1567	0.11	0.10	0.25	0.17	33	20							
	1640							0.17	0.23	0.23	0.09	15	5	
	1714	0.05	0.06	0.26	0.24	26	18							
G230L	2376	−0.01	0.03	0.25	0.20	74	26	0.00	0.07	0.27	0.20	77	24	0.04
G230M	1687	−0.01	0.01	0.24	0.19	35	26	0.02	0.03	0.23	0.17	35	18	0.02
	1933	0.00	0.00	0.20	0.19	30	24							
	2176	−0.02	−0.02	0.26	0.19	33	23							
	2419	−0.08	−0.07	0.22	0.20	23	18							
	2659	−0.10	−0.20	0.32	0.23	27	18							
	2898	−0.10	−0.11	0.25	0.24	15	9							
	3055	−0.23	−0.26	0.25	0.18	22	15	−0.19	−0.24	0.24	0.14	23	11	0.02
G230LB	2375	0.01	0.05	0.25	0.17	79	29	0.04	0.13	0.27	0.20	102	30	0.08
G230MB	1995	0.00	−0.01	0.19	0.13	60	33	−0.01	0.00	0.24	0.13	53	10	0.01
	2416	0.05	0.06	0.18	0.13	55	27	0.06	0.21	0.27	0.09	51	7	0.15
	2697	−0.05	−0.03	0.16	0.11	72	42	−0.01	0.11	0.24	0.09	55	12	0.14
	3115	0.03	−0.01	0.17	0.14	63	36	0.07	0.09	0.20	0.14	51	26	0.10
G430L	4300	−0.11	−0.12	0.26	0.17	74	20	−0.08	−0.11	0.25	0.20	82	23	0.01
G430M	3165	−0.04	−0.04	0.16	0.13	68	44	0.04	0.03	0.16	0.13	61	32	0.07
	3680	0.06	0.05	0.18	0.16	60	42	0.16	0.15	0.20	0.19	47	25	0.10
	4194	−0.17	−0.19	0.22	0.17	50	35							
	4961	−0.03	−0.05	0.15	0.10	38	31	0.03	0.03	0.18	0.09	30	19	0.08
	5471	0.06	0.05	0.14	0.11	26	24	0.13	0.15	0.16	0.07	22	12	0.10
G750L	7751	−0.21	−0.19	0.11	0.10	49	37	−0.09	−0.08	0.11	0.10	54	42	0.11
	8975	−0.12	−0.14	0.16	0.13	34	26							
G750M	5734	−0.06	−0.05	0.08	0.06	27	22	0.05	0.05	0.12	0.07	26	20	0.10
	6581	0.04	0.05	0.07	0.06	19	15							
	6768	−0.01	−0.02	0.10	0.09	13	10	0.07	0.08	0.03	0.03	10	9	0.10
	8311	0.00	−0.01	0.07	0.07	18	17	0.08	0.07	0.06	0.06	19	17	0.08
	8561	0.04	0.04	0.07	0.07	24	21							
	9336	−0.10	−0.09	0.11	0.11	30	27	0.04	0.05	0.12	0.09	20	15	0.14
	10363	−0.04	−0.04	0.21	0.21	8	8							

Notes: [a] For the subset of unblended lines measured in most of the cycles ("gnb").
[b] Difference in mean offset for cycles 17–25 versus cycles 7–11 (i.e., column 10 minus column 4).
Mean offsets and standard deviations are in pixels.
G140M/1173 data are from Spectroscopic Sensitivity and Focus Monitor programs

lines and changes in the relative line strengths. Further adjustments were made in cycle 25: (1) The G230MB/1713 setting was dropped, because there were too few detectable lines even in the relatively long exposures used for that setting, and because no GO programs have used the setting since SM4. (2) The total exposure times for G230MB/1995 and G230MB/2416 were increased, and multiple exposures were obtained in order to facilitate removal of cosmic rays. More reliable results are now obtained for those two settings. (3) The lamp for the E140H/1271 and G140M/1218 settings was changed from LINE to HITM2, to enable detection of more lines below 1270 Å. (4) The exposure times for several other settings were increased – yielding slight increases in the number of detected lines.

4. Conclusions / Recommendations

Examination of wavelength calibration spectra from cycles 7–11 and 17–25, using a refined, uniform analysis procedure and an expanded list of more accurate reference wavelengths, indicates that all of the monitored STIS first-order settings remain within the desired external and internal accuracies. For all of the first-order settings observed in cycle 25, the mean wavelength offsets for unblended lines (relative to the corresponding laboratory reference values) are ≤ 0.2 pixel, and the standard deviations of the residuals are < 0.3 pixel. There appears to have been a slight ($\sim$0.1 pixel) increase in the mean offsets for most of the first-order CCD settings in cycle 11, when the lamp used for the CCD calibrations was changed from LINE to HITM1; the mean offsets for some of the settings may exhibit weak secular trends. Consistently non-zero mean offsets and/or apparent trends of the residuals with wavelength for some of the settings – reminiscent of similar results found in analyses of STIS echelle spectra – suggest that the wavelength calibration could be improved. If the calibration lamps continue to fade at the current apparent rates (e.g., Peeples 2017; this study), the changes in the dispersion monitor programs made for cycles 24 and 25 should be sufficient to allow adequate monitoring of the STIS wavelength calibration for the next several cycles.

There are some issues concerning the wavelength calibration, however, that remain to be addressed:

- Similar analyses – examining the data from all available cycles versus the more extensive and accurate rest wavelengths now available – should be performed both for the MAMA echelle spectra and for CCD spectra obtained at the E1 pseudo-aperture.

- Given that work has begun on a "legacy archive" of STIS spectra, that some deficiencies in the current wavelength calibration have been noted (e.g., Valenti 1996; Ayres 2008, 2010a, 2010b; Pas11; Son15; this study), and that more extensive and accurate laboratory wavelengths are now available, revisions to the wavelength calibration should be considered. While adoption of a more physical, instrument-based model (e.g., Kerber et al. 2006a) would be desirable, much of the potential improvement in the calibration might be realized more simply by incorporating several additional terms in the dispersion relations (e.g., Ayres 2008, 2010a, 2010b).

- In connection with a re-calibration, it would be useful to obtain one more set of observations covering more of the available wavelength settings (e.g., as in cycles 11 and

17) – to reduce the interpolations and extrapolations of dispersion coefficients that would otherwise be necessary. Deeper exposures for some of the settings (e.g., Table 3 of Pas11) would increase the number of detectable lines – thus enabling more well determined fits to the dispersion relations for those settings.

- A more specific assigning of relative strengths to the lines from the different species in the reference wavelength list, based on the actual observations of the onboard Pt/Cr-Ne lamps used for the calibrations – extending the work of Ayres (2008, 2010a, 2010b) to longer wavelengths – would aid the evaluation of the CCD spectra.

- At present, the LINE lamp is still brighter than the HITM2 lamp longward of about 1270 Å, but the more rapid decline of the LINE lamp suggests that it might be useful to switch some of the other short-wavelength settings to HITM2 in the near future. The strengths of the lines in all three lamps, for different wavelength regimes, should be monitored.

- As the fading of the calibration lamps affects our ability to assess the calibration at the shortest wavelengths, it would be of interest to try to understand why those lamps are fading. While such severe time-dependent fading has not been seen in ground-based testing of similar lamps (e.g., Nave et al. 2012), an apparent fading at the shortest wavelengths seen in some tests was ascribed to degraded alignment and focus at those wavelengths (Kerber et al. 2006). Could such alignment/focus issues be at least partly responsible for the observed severe fading of the lamps at the shortest wavelengths? Is there any evidence for differences in the fading of lines from different species, or for any broadening of the lines with time?

- With the increases in exposure time adopted for some settings in cycle 25, there is no more time available in the usual allocation for these programs (3 internal orbits for the CCD, 7 internal orbits for the MAMA). It may be useful, however, to split more of the CCD exposures into two, in order to enable elimination of cosmic rays – Or, alternatively, to try to enhance the analysis code to do that for single exposures.

- At this point, all but one of the regularly monitored STIS settings use a lamp current of 10 mA. Increasing the current to 20 mA for settings where most of the lines are weak, while possible in principle, may not be desirable – as care would need to be taken to not saturate the MAMA detectors.

Acknowledgements

We thank D. Lindler for supplying the original line lists used for calibration and information on how that calibration was performed and P. Sonnentrucker for comments on the original version of this report. Various other members of the STIS team (especially P. Sonnentrucker, S. Lockwood, and T. Sohn) provided initial assistance with the analysis software.

Change History for STIS ISR 2018-04

Version 1: 2018 Aug 29 – original report

References

Ayres, T. R. 2008, ApJ, 177, 626

Ayres, T. R. 2010a, ApJS, 187, 149

Ayres, T. R. 2010b, in The 2010 Space Telescope Science Institute Calibration Workshop – Hubble after SM4. Preparing JWST, eds. S. Deustua & C. Oliveira, p. 57, Ironing Out the Wrinkles in STIS

Baum, S. 1997, STIS Instrument Science Report 1997-01, Automatic and GO Wavecals, for CCD and MAMA Spectroscopic Observations

Carlberg, J. K. & Monroe, T. 2017, STIS Instrument Science Report 2017-06, Updated Time Dependent Sensitivity Corrections for STIS Spectral Modes

Espey, B. 1999, STIS Technical Instrument Report 1999-03, Revised Dispersion Solution Software

Friedman, S. D. 2005, STIS Instrument Science Report 2005-03, Wavelength Calibration Accuracy of the First-Order CCD Modes Using the E1 Aperture

Hodge, P., Baum, S., McGrath, M., Hulbert, S., & Christensen, J. 1998, STIS Instrument Science Report 1998-12, Calstis4, calstis11, calstis12: Wavecal Processing in the STIS Calibration Pipeline

Hulbert, S, Hodge, P., & Baum, S. 1996, STIS Instrument Science Report 1996-019, The STScI STIS Pipeline VI: Reduction of WAVECALs

Hulbert, S., Hodge, P., & Busko, I. 1997, STIS Instrument Science Report 1997-02, The STScI STIS Pipeline VII: Extraction of 1-D Spectra

Kerber, F., Rosa, M. R., Sansonetti, C. J., et al. 2004, Proc. SPIE, 5488, 679

Kerber, F., Bristow, P., & Rosa, M. R. 2006a, in The 2005 HST Calibration Workshop, eds. A. M. Koekemoer, P. Goudfrooij, & L. L. Dressel, p. 309, STIS Calibration Enhancement (STIS-CE): Dispersion Solutions Based on a Physical Instrument Model

Kerber, F., Bristow, P., Rosa, M. R., et al. 2006b, in The 2005 HST Calibration Workshop, eds. A. M. Koekemoer, P. Goudfrooij, & L. L. Dressel, p. 318, Characterization of Pt/Cr-Ne Hollow-Cathode Lamps for Wavelength Standards in Space Astronomy

Kramida, A. E. & Nave, G. 2006a, Eur. Phys. J. D, 37, 1

Kramida, A. E. & Nave, G. 2006b, Eur. Phys. J. D, 39, 331

Lindler, D. 1999, STIS IDT Post-Launch Analysis Report #062, Echelle Wavelength Calibration Update

McGrath, M., Busko, & Hodge, P. 1999, STIS Instrument Science Report 1999-03, Calstis6: Extraction of 1-D Spectra in the STIS Calibration Pipeline

Nave, G., Sansonetti, C. J., Kerber, F., et al. 2008, Proc. SPIE, 7011, 3L

Nave, G., Sansonetti, C. J., Penton, S. V., et al. 2012, PASP, 124, 1295

Pascucci, I., Proffitt, C., Ghavamian, P., et al. 2010a, STIS Instrument Science Report 2010-10, Monitoring of the Wavelength Calibration Lamps for the Hubble Space Telescope

Pascucci, I., Proffitt, C., Ghavamian, P., et al. 2010b, Proc. SPIE, 7731, 3B
Pascucci, I., Proffitt, C. R., Ghavamian, P., et al. 2010c, in The 2010 Space Telescope Science Institute Calibration Workshop – Hubble after SM4. Preparing JWST, eds. S. Deustua & C. Oliveira. p. 439, Monitoring of the Wavelength Calibration Lamps for the Hubble Space Telescope
Pascucci, I., Hodge, P., Proffitt, C. R., & Ayres, T. 2011, STIS Instrument Science Report 2011-01, Wavelength Calibration Accuracy for the STIS CCD and MAMA Modes (Pas11)
Peeples, M. 2017, STIS Instrument Science Report 2017-04, On the Fading of the STIS Ultraviolet Calibration Lamps
Reader, J., Acquista, N., Sansonetti, C. J., & Sansonetti, J. E. 1990, ApJS, 72, 831
Sansonetti, C. J., Kerber, F., Reader, J., & Rosa, M. R. 2004, ApJS, 153, 555
Sansonetti, C. J. & Nave, G. 2014, ApJS, 213, 28
Sansonetti, C. J., Nave, G., Reader, J., & Kerber, F. 2012, ApJS, 202, 15
Smith, M. A. 1990, in Evolution in Astrophysics: IUE Astronomy in the Era of New Space Missions, ed. E. J. Rolfe, ESA SP-310, p. 627, A Revised Parameterization of the Dispersion Constants for High Dispersion IUE Images
Sonnentrucker, P. 2015, STIS Instrument Science Report 2015-02, Multi-Cycle Analysis of the STIS Dispersion Solutions (Son15)
Valenti, J. A. 1966, STIS IDT Pre-Launch Analysis Report #072, Current Status of STIS Echelle Wavelength Solutions
Wallace, L. & Hinkle, K. 2009, ApJ, 700, 720

STIS team calibration close-out Instrument Science Reports:

cycle 7: Dashevsky, I., & McGrath, M. A. 2000, STIS ISR 2000-04
cycle 8: Diaz-Miller, R. I., & Goudfrooij, P. 2001, STIS ISR 2001-04
cycle 9: Proffitt, C. R., & Davies, J. 2003, STIS ISR 2003-02
cycle 10: Dressel, L., & Davies, J. 2004, STIS ISR 2004-06
cycle 17: Wolfe, M. A., Osten, R. A., Aloisi, A. et al. 2012, STIS ISR 2012-03
cycle 18: Kriss, G. A., Wolfe, M. A., Aloisi, A. et al. 2013, STIS ISR 2013-03
cycle 19: Roman-Duval, J., Ely, J., Aloisi, A. et al. 2014, STIS ISR 2014-01
cycle 20: Roman-Duval, J., Ely, J., Cox, C. et al. 2015, STIS ISR 2015-08
cycle 21: Sana, H., Fox, A., Roman-Duval, J. et al. 2015, STIS ISR 2015-09

Appendices

- Figure 6 – wavelength differences between the LindPC list and the current NIST values
- Figures 7–11 – average wavelength residuals (observed minus reference) for individual lines in settings monitored for all five STIS gratings during cycles 7–11
- Tables 5–6 – detailed mean wavelength offset values for the MAMA and CCD settings monitored in each cycle

- Tables 7–8 – standard deviations of the wavelength residuals for the MAMA and CCD settings monitored in each cycle
- Table 9 – strengths of emission lines, generally relative to the values in cycles 7 and 17, for the MAMA and CCD settings monitored in each cycle
- Tables 10–11 – number of unblended lines measured for the MAMA and CCD settings monitored in each cycle
- Table 12 – comparison of mean wavelength offsets, scatter in the residuals, and number of lines measured for the MAMA and CCD settings monitored in cycle 17 (versus Pas11) and in cycles 19–21 (versus Son15)

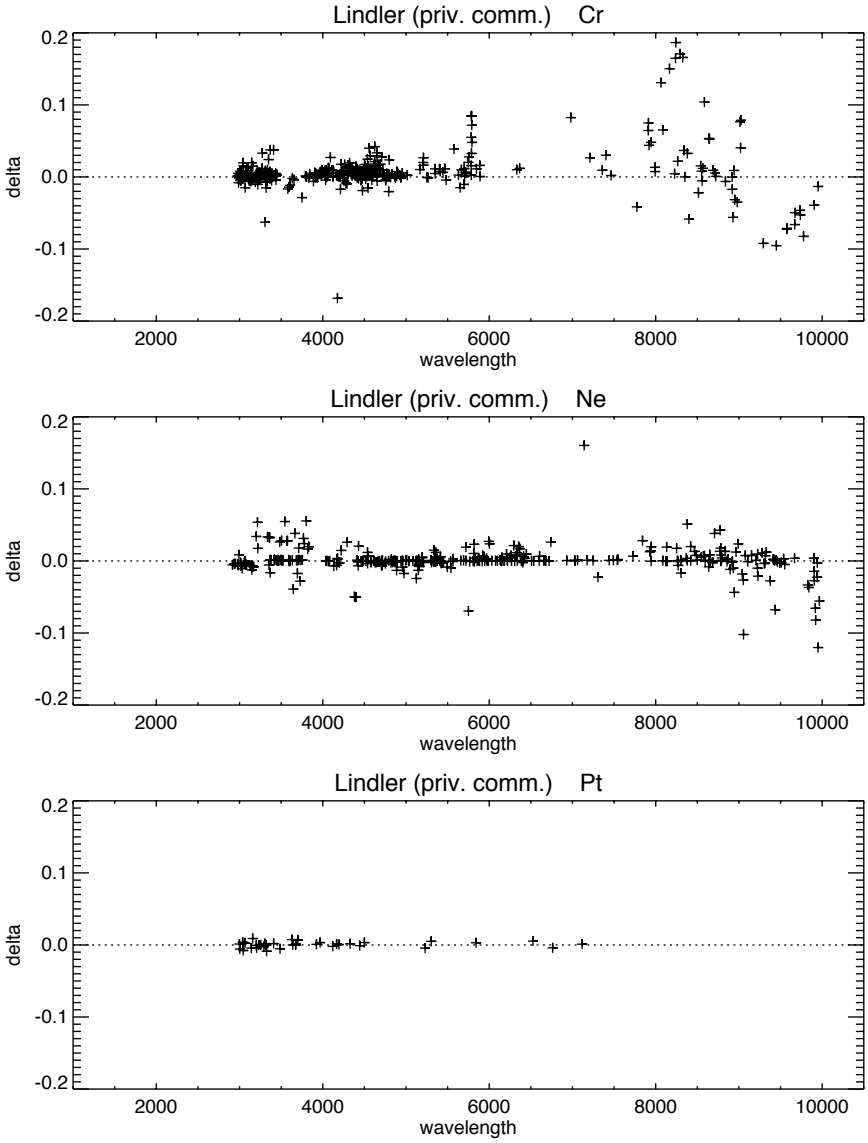

Figure 7: Differences in reference wavelengths (in Å): LindPC line list (similar to the original STIS line list; Lindler, private communication) vs. current NIST values. While there are large (tens of mÅ) differences for many Cr and Ne lines at the longer wavelengths, many of the larger differences are for relatively weak lines. For comparison, one pixel corresponds to 2.73 Å for G430L, 0.28 Å for G430M, 4.92 Å for G750L, and 0.56 Å for G750M. Note that the current NIST values for Pt need updating.

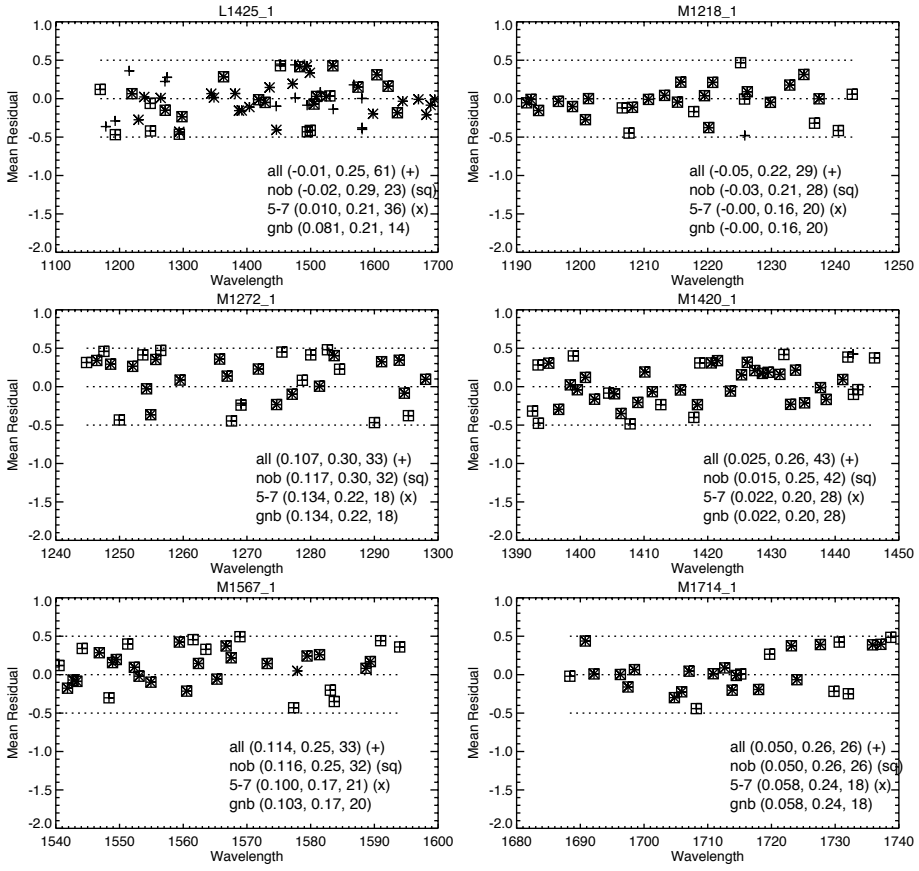

Figure 8: Average residuals (in pixels) for individual lines measured in G140L and G140M settings monitored in cycles 7–11. In each case, lines measured in any cycle (all) are given by "+"; unblended lines (nob) are given by open squares; and lines measured in at least five of the seven data sets (5-7) are given by "x"; the most reliable lines (gnb) are thus given by a superposition of all three symbols. The mean average offset, the standard deviation, and the number of points for each of those are given in the lower right-hand corner of each panel. For the most reliable lines, the mean offsets range from 0.00 to 0.13 pix; the standard deviations are all less than 0.25 pix.

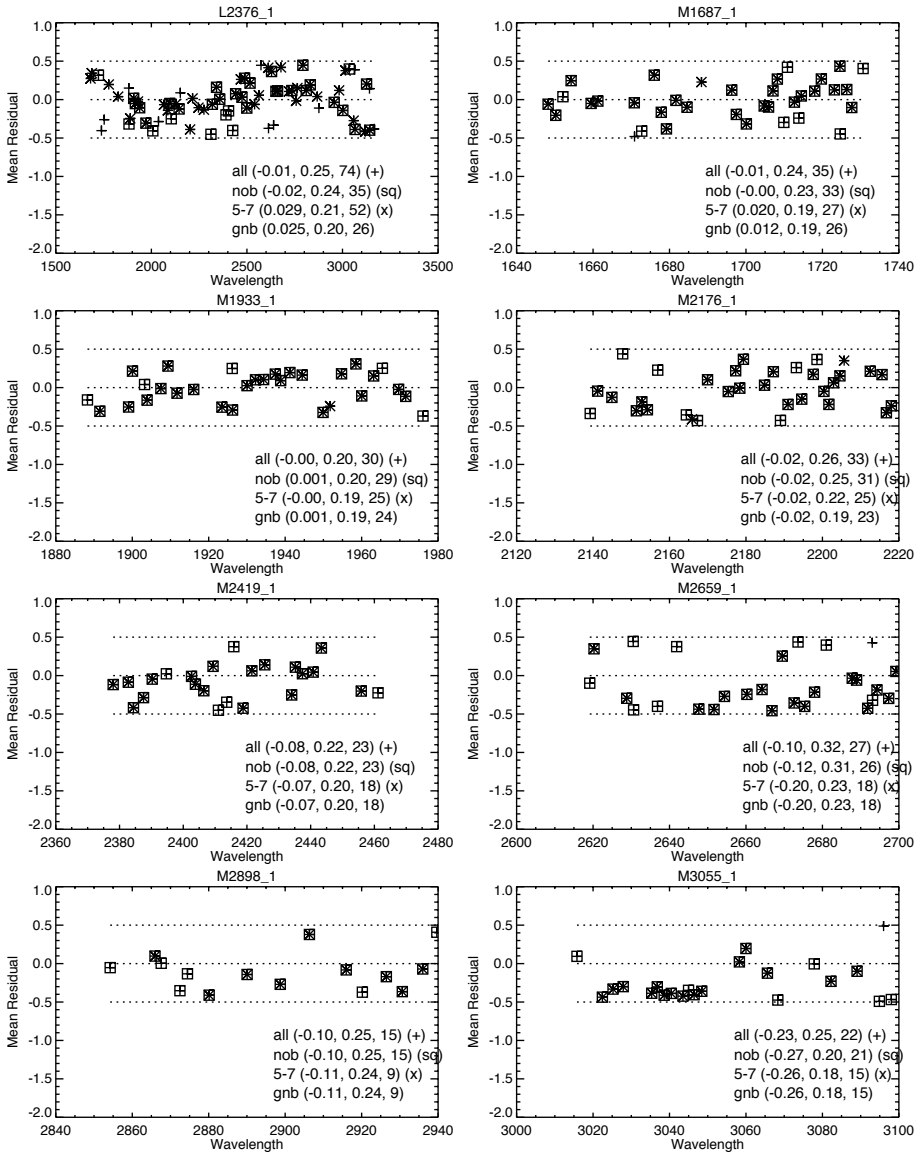

Figure 9: Average residuals (in pixels) for individual lines measured in G230L and G230M settings monitored in cycles 7–11. In each case, lines measured in any cycle (all) are given by "+"; unblended lines (nob) are given by open squares; and lines measured in at least five of the seven data sets (5-7) are given by "x"; the most reliable lines (gnb) are thus given by a superposition of all three symbols. The mean average offset, the standard deviation, and the number of points for each of those are given in the lower right-hand corner of each panel. For the most reliable lines, the mean offsets range from −0.20 to 0.03 pix; the standard deviations are all less than 0.25. Note the systematic trends in the average residuals, as functions of wavelength, for some settings (especially L2376).

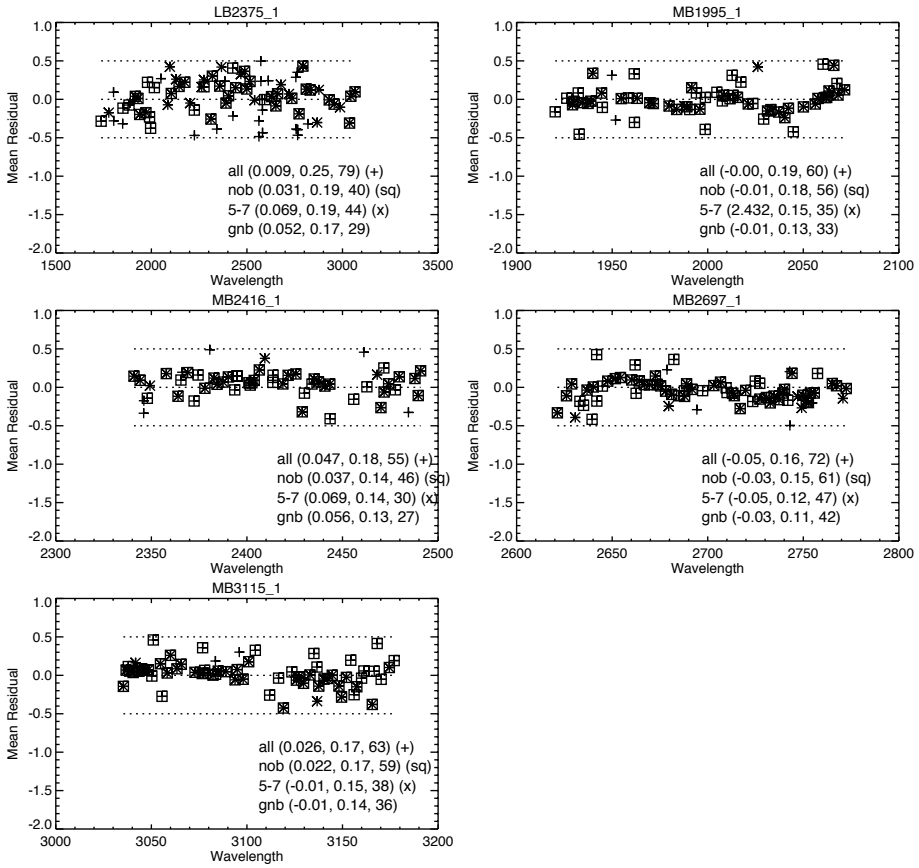

Figure 10: Average residuals (in pixels) for individual lines measured in G230LB and G230MB settings monitored in cycles 7–11. In each case, lines measured in any cycle (all) are given by "+"; unblended lines (nob) are given by open squares; and lines measured in at least five of the seven data sets (5-7) are given by "x"; the most reliable lines (gnb) are thus given by a superposition of all three symbols. The mean average offset, the standard deviation, and the number of points for each of those are given in the lower right-hand corner of each panel. For the most reliable lines, the mean offsets range from -0.03 to 0.06 pix; the standard deviations are all less than 0.20. Note the systematic trends in the average residuals, as functions of wavelength, for some settings (especially MB1995 and MB2697).

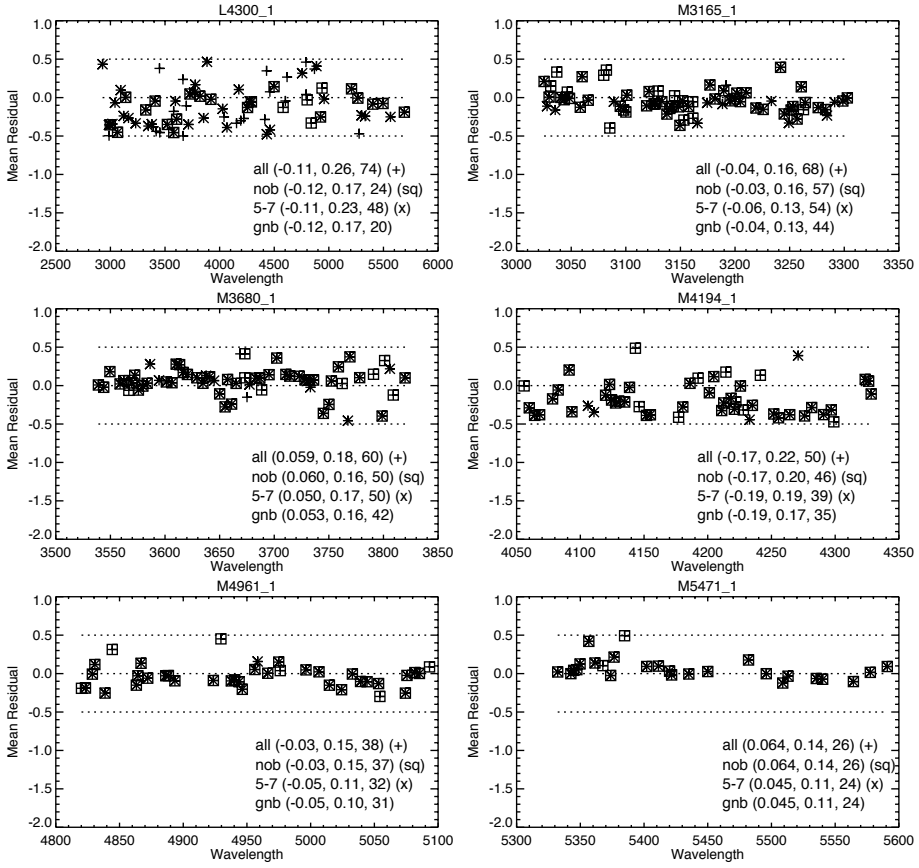

Figure 11: Average residuals (in pixels) for individual lines measured in G430L and G430M settings monitored in cycles 7–11. In each case, lines measured in any cycle (all) are given by "+"; unblended lines (nob) are given by open squares; and lines measured in at least five of the seven data sets (5-7) are given by "x"; the most reliable lines (gnb) are thus given by a superposition of all three symbols. The mean average offset, the standard deviation, and the number of points for each of those are given in the lower right-hand corner of each panel. For the most reliable lines, the mean offsets range from -0.19 to 0.05 pix; the standard deviations are all less than 0.20. Note the systematic trends in the average residuals, as functions of wavelength, for some settings (especially M5471).

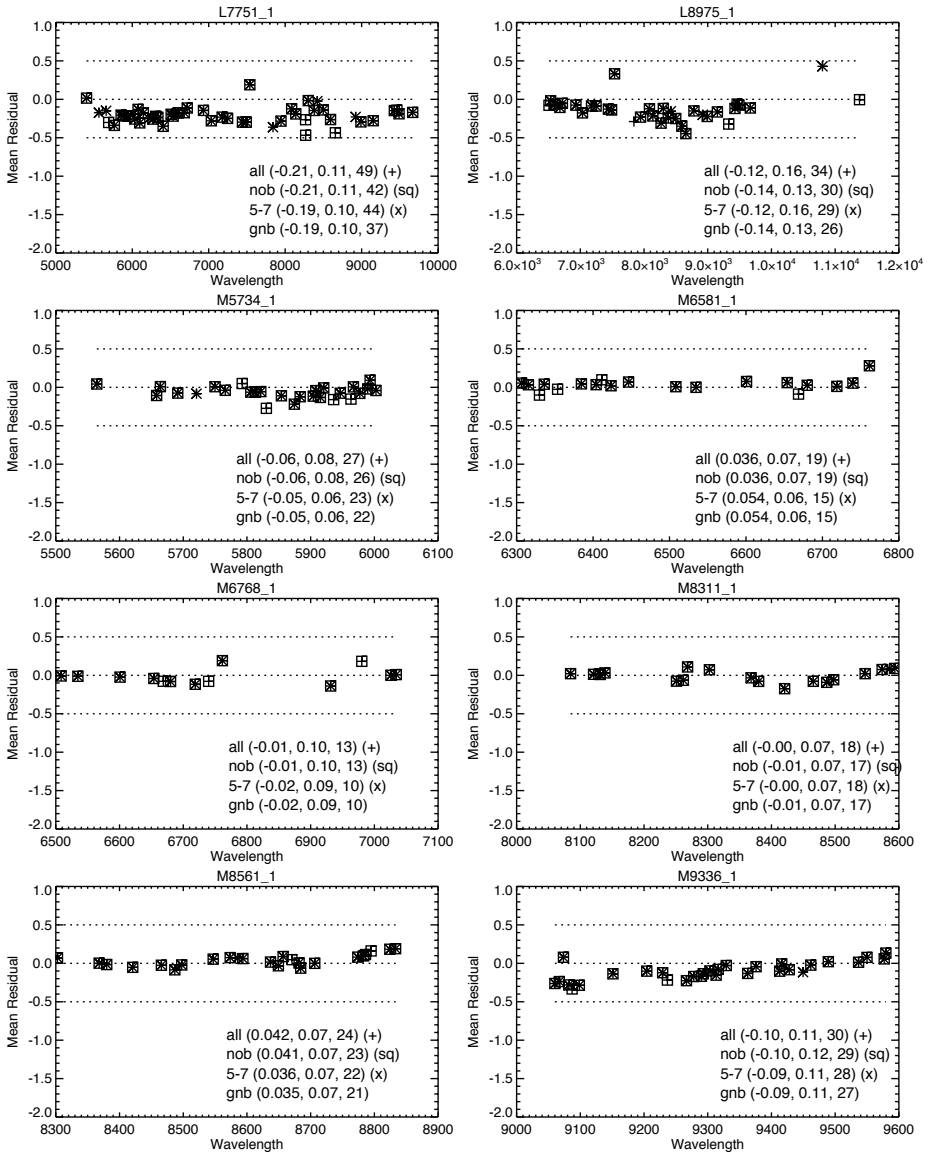

Figure 12: Average residuals (in pixels) for individual lines measured in G750L and G750M settings monitored in cycles 7–11. In each case, lines measured in any cycle (all) are given by "+"; unblended lines (nob) are given by open squares; and lines measured in at least five of the seven data sets (5-7) are given by "x"; the most reliable lines (gnb) are thus given by a superposition of all three symbols. The mean average offset, the standard deviation, and the number of points for each of those are given in the lower right-hand corner of each panel. For the most reliable lines, the mean offsets range from −0.19 to 0.05 pix; the standard deviations are all less than 0.15. Note the systematic trends in the average residuals, as functions of wavelength, for some settings (especially M8311 and M9336).

Table 5: Monitored settings: mean offsets (first-order MAMA; in pixels)

Grating	Wave	7a	7b	8a	8b	9	10	11	17	18	19	20	21	22	23	24	25
G140L	1425	0.02	0.03	0.00	0.06	0.03	0.05	0.01	0.09	-0.02	0.04	0.11	0.13	0.02	0.00	-0.13	-0.11
G140M	1173							0.00			-0.02	0.00	-0.07	0.00	-0.05	0.01	0.00
	1218	0.00	-0.01	0.05	-0.02	0.01	-0.08	-0.03	0.06	-0.07	-0.01	-0.05	-0.03	-0.11	-0.06	-0.02	-0.02
	1222							0.01	0.16								
	1272	0.12	0.13	0.13	0.10	0.13	0.09	0.10									
	1321							0.05	0.02								
	1371							0.00									
	1387							0.09									
	1400							0.15									
	1420	0.00	0.02	0.06	0.01	0.06	0.05	0.03	0.03								
	1470							0.07									
	1518							0.05									
	1540							0.14	0.10								
	1550							0.21									
	1567	0.13	0.09	0.11	0.06	0.12	0.11	0.07									
	1616							0.05									
	1640							0.15	0.24	0.18	0.24	0.18	0.11	0.26	0.09	0.18	0.18
	1665							0.11									
	1714	-0.01	0.07	0.10	0.05	0.09	0.04	0.00									
G230L	2376	-0.03	0.04	0.00	0.06	0.01	-0.03	0.00	0.00	0.06	0.02	0.02	0.07	0.03	0.08	0.08	0.01
G230M	1687	-0.02	0.01	0.00	0.03	0.00	0.00	-0.01	0.08	0.01	-0.02	0.03	0.03	0.01	-0.02	0.00	-0.01
	1769							-0.12									
	1851							-0.05									
	1884							-0.13									
	1933	0.00	0.01	0.00	0.00	0.04	-0.02	0.00									
	2014							-0.13									
	2095							-0.15									
	2176	-0.01	-0.05	-0.01	0.02	-0.04	-0.03	-0.03									
	2257							-0.08									
	2338							-0.13	-0.09								
	2419	0.00	-0.10	-0.06	-0.09	-0.01	-0.07	-0.08									
	2499							-0.10									
	2579							0.10									
	2600							-0.08									
	2659	-0.08	-0.16	-0.19	-0.16	-0.24	-0.15	-0.18									
	2739							-0.16									
	2800							-0.05									
	2818							-0.09	-0.23								
	2828							-0.19									
	2898	-0.14	-0.12	-0.06	-0.08	-0.24	-0.13	-0.08									
	2977							-0.20									
	3055	-0.27	-0.28	-0.23	-0.22	-0.23	-0.33	-0.24	-0.21	-0.31	-0.18	-0.27	-0.20	-0.22	-0.21	-0.11	-0.20

Notes: Lamp current for G140L/1425 and G230M/3055 was increased from 3.8 to 10 mA in cycle 24.
Lamp for G140M/1218 was switched from LINE to HITM2 in cycle 25.
G140M/1173 data are from Spectroscopic Sensitivity and Focus Monitor programs

Table 6: Monitored settings: mean offsets (first-order CCD; in pixels)

Grating	Wave	7a	7b	8a	8b	9	10	11	17	18	19	20	21	22	23	24	25
G230LB	2375	0.04	0.04	0.05	0.05	0.04	0.00	0.13	0.05	0.11	0.14	0.13	0.05	0.17	0.11	0.16	0.10
G230MB	1854							0.00	0.07								
	1995	-0.03	0.01	0.01	0.00	-0.01	-0.03	0.09	0.02	0.03	0.00	0.00	-0.02	-0.03	-0.01	0.05	0.08
	2135							0.09	-0.07								
	2276							-0.07	0.01								
	2416	-0.01	0.03	0.06	0.11	0.06	0.04	0.16	0.19	0.14	0.11	0.10	0.05	0.25	0.17	0.07	0.18
	2557							-0.01	-0.12								
	2697	0.00	-0.06	-0.03	0.03	-0.03	-0.06	0.00	0.07	0.00	0.00	0.07	0.08	0.09	0.13	0.01	0.05
	2794							0.05	0.09								
	2836							0.12	0.09								
	2976							0.25	0.26								
	3115	-0.02	0.00	0.03	0.05	0.02	-0.02	0.10	0.17	0.02	0.12	0.16	0.06	0.06	0.06	0.04	0.08
G430L	4300	-0.15	-0.11	-0.12	-0.10	-0.12	-0.13	-0.14	-0.16	-0.14	-0.04	-0.13	-0.07	-0.12	-0.03	-0.04	-0.05
G430M	3165	-0.07	-0.07	-0.02	0.00	-0.04	-0.05	-0.03	0.04	0.02	0.06	0.00	0.01	0.05	0.06	0.07	0.04
	3423							0.10	0.11								
	3680	0.03	0.03	0.07	0.11	0.06	0.03	0.11	0.15	0.14	0.19	0.17	0.14	0.16	0.18	0.17	0.17
	3843							0.04	0.07								
	3936							0.06	0.06								
	4194	-0.17	-0.16	-0.17	-0.22	-0.16	-0.19	-0.20	-0.17								
	4451							0.09	0.08								
	4706							0.15	0.13								
	4961	-0.10	-0.07	-0.01	-0.02	-0.03	-0.05	0.00	-0.02	-0.01	-0.05	0.07	0.04	0.05	0.08	0.05	-0.03
	5093							0.08	0.05								
	5216							0.01	0.03								
	5471	0.01	0.05	0.05	0.07	0.05	0.04	0.15	0.15	0.06	0.18	0.14	0.16	0.11	0.17	0.13	0.16
G750L	7751	-0.23	-0.22	-0.20	-0.19	-0.20	-0.17	-0.03	-0.12	-0.11	-0.09	-0.03	-0.12	-0.02	-0.10	-0.01	-0.09
	8975	-0.13	-0.15	-0.14	-0.09	-0.10	-0.19										
G750M	5734	-0.10	-0.06	-0.06	-0.02	-0.02	-0.08	0.06	0.03	0.10	0.05	0.05	0.02	0.09	0.06	0.09	0.05
	6252							0.17	0.12								
	6581	0.05	0.04	0.04	0.06	0.06	0.04	0.18	0.17								
	6768	-0.09	-0.01	-0.02	0.01	-0.01	-0.01	0.05	0.06	0.08	0.05	0.08	0.06	0.12	0.07	0.09	0.10
	7283							0.10	0.11								
	7795							0.17	0.17								
	8311	-0.05	0.00	0.00	0.04	-0.02	-0.03	0.10	0.12	0.09	0.07	0.06	0.04	0.04	0.05	0.07	0.05
	8561	0.02	0.01	0.03	0.08	0.04	0.05	0.16	0.10								
	8825							0.16	0.15								
	9336	-0.08	-0.07	-0.10	-0.09	-0.09	-0.13	0.03	0.05	0.00	0.08	0.07	0.08	0.07	0.01	0.02	0.09
	9851							-0.01	0.10								
	10363	0.06	-0.07	-0.01	-0.04	-0.12	-0.06										

Notes: Lamp for all CCD settings switched from LINE to HITM1 in cycle 11.
Multiple exposures obtained for G230MB/1995 and G230MB/2416 in cycle 25.

Table 7: Monitored settings: standard deviations (first-order MAMA; in pixels)

Grating	Wave	7a	7b	8a	8b	9	10	11	17	18	19	20	21	22	23	24	25
G140L	1425	0.29	0.33	0.23	0.22	0.25	0.22	0.23	0.23	0.25	0.25	0.19	0.26	0.31	0.24	0.20	0.21
G140M	1173							0.14			0.23	0.28	0.27	0.18	0.24	0.21	0.23
	1218	0.19	0.17	0.20	0.23	0.21	0.15	0.16	0.21	0.24	0.25	0.20	0.24	0.13	0.23	0.27	0.18
	1222							0.30	0.27								
	1272	0.27	0.27	0.31	0.27	0.29	0.28	0.25									
	1321							0.27	0.29								
	1371							0.24									
	1387							0.22									
	1400							0.27									
	1420	0.25	0.24	0.23	0.21	0.24	0.20	0.23	0.21								
	1470							0.24									
	1518							0.23									
	1540							0.17	0.24								
	1550							0.22									
	1567	0.24	0.20	0.22	0.20	0.23	0.23	0.22									
	1616							0.29									
	1640							0.22	0.19	0.30	0.17	0.28	0.28	0.07	0.31	0.09	0.29
	1665							0.20									
	1714	0.30	0.27	0.25	0.28	0.21	0.25	0.25									
G230L	2376	0.23	0.20	0.22	0.19	0.20	0.20	0.21	0.21	0.23	0.21	0.23	0.22	0.22	0.21	0.20	0.24
G230M	1687	0.22	0.23	0.23	0.19	0.24	0.21	0.23	0.21	0.24	0.20	0.24	0.19	0.16	0.23	0.20	0.18
	1769							0.23									
	1851							0.20									
	1884							0.18									
	1933	0.18	0.18	0.20	0.21	0.23	0.19	0.19									
	2014							0.18									
	2095							0.21									
	2176	0.22	0.23	0.21	0.24	0.23	0.25	0.27									
	2257							0.23									
	2338							0.20	0.21								
	2419	0.19	0.25	0.22	0.22	0.21	0.20	0.18									
	2499							0.21									
	2579							0.21									
	2600							0.28									
	2659	0.28	0.29	0.25	0.28	0.19	0.29	0.28									
	2739							0.20									
	2800							0.20									
	2818							0.24	0.14								
	2828							0.23									
	2898	0.19	0.22	0.23	0.27	0.17	0.23	0.28									
	2977							0.13									
	3055	0.22	0.17	0.20	0.27	0.23	0.13	0.18	0.22	0.17	0.21	0.19	0.19	0.20	0.17	0.28	0.21

Notes: Lamp current for G140L/1425 and G230M/3055 was increased from 3.8 to 10 mA in cycle 24.
Lamp for G140M/1218 was switched from LINE to HITM2 in cycle 25.
G140M/1173 data are from Spectroscopic Sensitivity and Focus Monitor programs

Table 8: Monitored settings: standard deviations (first-order CCD; in pixels)

Grating	Wave	7a	7b	8a	8b	9	10	11	17	18	19	20	21	22	23	24	25
G230LB	2375	0.18	0.18	0.20	0.17	0.20	0.18	0.23	0.17	0.18	0.24	0.21	0.21	0.17	0.25	0.20	0.23
G230MB	1854							0.26	0.22								
	1995	0.15	0.17	0.16	0.16	0.14	0.17	0.20	0.25	0.15	0.17	0.27	0.18	0.23	0.20	0.22	0.17
	2135							0.17	0.19								
	2276							0.20	0.22								
	2416	0.15	0.15	0.11	0.13	0.19	0.16	0.10	0.14	0.17	0.22	0.25	0.28	0.13	0.16	0.30	0.19
	2557							0.24	0.17								
	2697	0.09	0.14	0.16	0.14	0.14	0.15	0.18	0.22	0.19	0.23	0.21	0.14	0.18	0.22	0.18	0.19
	2794							0.16	0.20								
	2836							0.20	0.22								
	2976							0.19	0.13								
	3115	0.18	0.16	0.15	0.16	0.15	0.16	0.18	0.17	0.16	0.19	0.17	0.17	0.19	0.19	0.17	0.17
G430L	4300	0.17	0.17	0.18	0.17	0.18	0.16	0.21	0.22	0.20	0.21	0.20	0.23	0.22	0.22	0.22	0.20
G430M	3165	0.15	0.13	0.16	0.16	0.14	0.13	0.17	0.16	0.13	0.15	0.16	0.16	0.16	0.12	0.15	0.14
	3423							0.11	0.11								
	3680	0.15	0.16	0.16	0.16	0.16	0.17	0.21	0.18	0.21	0.19	0.20	0.21	0.18	0.19	0.17	0.23
	3843							0.18	0.16								
	3936							0.17	0.13								
	4194	0.21	0.22	0.17	0.19	0.21	0.18	0.18	0.15								
	4451							0.21	0.19								
	4706							0.21	0.21								
	4961	0.10	0.12	0.15	0.12	0.11	0.12	0.16	0.14	0.14	0.13	0.17	0.11	0.13	0.14	0.10	0.14
	5093							0.22	0.18								
	5216							0.16	0.17								
	5471	0.13	0.15	0.09	0.07	0.08	0.14	0.11	0.09	0.17	0.07	0.15	0.12	0.22	0.11	0.11	0.09
G750L	7751	0.10	0.11	0.11	0.10	0.11	0.11	0.11	0.11	0.10	0.11	0.10	0.11	0.10	0.10	0.12	0.11
	8975	0.14	0.13	0.14	0.15	0.14	0.12										
G750M	5734	0.07	0.06	0.07	0.07	0.09	0.05	0.10	0.11	0.07	0.11	0.09	0.07	0.10	0.07	0.09	0.08
	6252							0.07	0.09								
	6581	0.05	0.07	0.09	0.12	0.07	0.06	0.09	0.07								
	6768	0.05	0.09	0.07	0.06	0.08	0.18	0.03	0.03	0.03	0.03	0.03	0.03	0.03	0.03	0.03	0.03
	7283							0.05	0.04								
	7795							0.10	0.15								
	8311	0.07	0.07	0.07	0.07	0.07	0.07	0.06	0.06	0.06	0.06	0.06	0.06	0.09	0.06	0.08	0.07
	8561	0.07	0.07	0.09	0.07	0.07	0.07	0.06	0.07								
	8825							0.05	0.12								
	9336	0.16	0.12	0.13	0.11	0.11	0.12	0.12	0.09	0.10	0.14	0.12	0.12	0.11	0.09	0.10	0.12
	9851							0.18	0.08								
	10363	0.25	0.19	0.21	0.17	0.20	0.26										

Notes: Lamp for all CCD settings switched from LINE to HITM1 in cycle 11.
Multiple exposures obtained for G230MB/1995 and G230MB/2416 in cycle 25.

Table 9: Monitored settings: relative line strengths (first-order MAMA and CCD)

Grating	Wave	7a	7b	8a	8b	9	10	11	17	18	19	20	21	22	23	24	25
G140L	1425	1.00	0.91	0.68	0.60	0.61	0.55	0.52	1.00	0.89	0.82	0.78	0.74	0.67	0.68	...	...
G140M	1173										1.00	0.83	0.75	0.69	0.61	0.56	0.54
	1218	1.00	0.90	0.70	0.55	0.57	0.41	0.37	1.00	0.75	0.55	0.42	0.34	0.28	0.26	0.27	...
	1272	1.00	0.95	0.76	0.65	0.66	0.57	0.49									
	1420	1.00	0.93	0.74	0.66	0.66	0.61	0.56									
	1567	1.00	0.90	0.66	0.59	0.61	0.50	0.49									
	1640							1.18	1.00	0.90	0.81	0.78	0.76	0.70	0.73	0.68	0.71
	1714	1.00	0.87	0.59	0.51	0.54	0.44	0.42									
G230L	2376	1.00	0.90	0.87	0.83	0.82	0.70	0.61	1.00	0.97	0.89	0.87	0.80	0.77	0.74	0.74	0.70
G230M	1687	1.00	0.90	0.89	0.74	0.74	0.71	0.62	1.00	0.93	0.88	0.87	0.80	0.76	0.73	0.67	0.68
	1933	1.00	0.87	0.87	0.70	0.71	0.57	0.49									
	2176	1.00	0.90	0.95	0.80	0.82	0.65	0.58									
	2419	1.00	0.91	0.95	0.86	0.88	0.71	0.62									
	2659	1.00	0.91	0.95	0.91	0.93	0.76	0.74									
	2898	1.00	0.92	0.94	0.95	0.96	0.74	0.77									
	3055	1.00	0.93	0.93	0.98	0.98	0.80	0.78	1.00	0.93	0.85	0.82	0.77	0.76	0.72	...	...
G230LB	2375	1.00	1.00	1.04	0.94	0.96	0.87	1.06	1.00	0.96	0.95	0.93	0.91	0.90	0.88	0.87	0.84
G230MB	1995	1.00	0.97	0.97	0.81	0.79	0.66	1.20	1.00	0.97	0.95	0.88	0.88	0.86	0.86	0.84	0.80
	2416	1.00	1.00	1.03	0.92	0.90	0.79	1.16	1.00	1.01	1.00	0.87	0.90	0.94	0.89	0.86	0.88
	2697	1.00	0.98	1.02	0.94	0.91	0.88	1.08	1.00	1.02	0.97	0.88	0.89	0.90	0.88	0.84	0.84
	3115	1.00	1.01	1.05	0.97	0.96	0.93	1.05	1.00	0.97	0.96	0.92	0.92	0.92	0.91	0.88	0.87
G430L	4300	1.00	0.98	1.06	1.04	1.05	0.97	1.06	1.00	1.00	0.99	1.00	0.99	0.97	0.95	0.96	0.97
G430M	3165	1.00	0.98	1.04	0.97	0.97	0.91	1.05	1.00	0.98	0.97	0.95	0.93	0.94	0.92	0.90	0.89
	3680	1.00	0.96	1.04	1.01	1.01	0.92	1.04	1.00	0.99	0.97	0.97	0.95	0.95	0.93	0.92	0.93
	4194	1.00	0.98	1.07	1.07	1.07	0.95										
	4961	1.00	1.00	1.06	1.05	1.05	1.01	1.02	1.00	1.02	0.99	0.99	0.97	1.00	0.99	0.97	0.96
	5471	1.00	1.00	1.06	1.04	1.03	1.00	0.99	1.00	1.00	1.00	1.00	0.99	0.99	0.98	0.97	0.97
G750L	7751	1.00	1.03	1.04	1.04	1.03	1.02	0.98	1.00	0.99	1.00	0.99	0.99	0.99	0.98	0.98	0.98
	8975																
G750M	5734	1.00	1.02	1.03	1.02	1.01	1.01	0.98	1.00	0.99	0.99	0.99	0.99	0.99	0.98	0.98	0.97
	6581	1.00	1.02	1.03	1.02	1.02	1.00										
	6768	1.00	1.02	1.03	1.02	1.02	1.01	0.99	1.00	0.99	0.99	0.99	0.98	0.98	0.98	0.98	0.97
	8311	1.00	1.02	1.03	1.02	1.02	1.00	0.98	1.00	1.00	1.00	1.00	1.00	1.00	0.99	0.99	0.98
	8561	1.00	1.01	1.04	1.02	1.02	0.99										
	9336	1.00	1.02	1.04	1.03	1.02	1.00	0.97	1.00	0.98	1.00	1.00	1.00	1.00	1.00	1.00	0.99
	10363	1.00															

Notes: Lamp current for G140L/1425 and G230M/3055 was increased from 3.8 to 10 mA in cycle 24.
Lamp for G140M/1218 was switched from LINE to HITM2 in cycle 25.
G140M/1173 data are from Spectroscopic Sensitivity and Focus Monitor programs
Lamp for all CCD settings switched from LINE to HITM1 in cycle 11; values for CCD in cycle 11 are relative to cycle 17.
Multiple exposures were obtained for G230MB/1995 and G230MB/2416 in cycle 25.

Table 10: Monitored settings: number of lines (first-order MAMA)

Grating	Wave	7a	7b	8a	8b	9	10	11	17	18	19	20	21	22	23	24	25
G140L	1425	18	20	14	15	17	17	14	15	18	14	13	13	14	13	22	16
G140M	1173							14			13	12	12	10	9	11	12
	1218	21	20	20	20	23	21	18	13	13	12	10	11	11	10	6	21
	1222							22	10								
	1272	25	23	20	20	25	20	19									
	1321							21	22								
	1371							31									
	1387							30									
	1400							28									
	1420	30	29	33	32	29	23	26	26								
	1470							25									
	1518							24									
	1540							19	24								
	1550							22									
	1567	22	20	24	18	24	22	22									
	1616							15									
	1640							13	7	7	7	10	7	5	10	5	8
	1665							19									
	1714	20	19	16	18	16	19	17									
G230L	2376	28	29	28	28	27	26	27	23	26	24	28	26	27	26	27	27
G230M	1687	28	27	28	24	26	28	27	18	18	20	24	23	21	24	24	19
	1769							19									
	1851							25									
	1884							18									
	1933	24	21	25	20	24	23	23									
	2014							23									
	2095							23									
	2176	23	23	25	26	26	23	24									
	2257							18									
	2338							17	16								
	2419	17	20	19	20	19	20	17									
	2499							22									
	2579							10									
	2600							13									
	2659	17	19	20	17	19	17	18									
	2739							15									
	2800							16									
	2818							13	7								
	2828							12									
	2898	8	11	9	12	11	10	8									
	2977							13									
	3055	15	15	14	16	18	14	18	10	11	11	16	13	13	15	12	12

Notes: Lamp current for G140L/1425 and G230M/3055 was increased from 3.8 to 10 mA in cycle 24.
Lamp for G140M/1218 was switched from LINE to HITM2 in cycle 25.
G140M/1173 data are from Spectroscopic Sensitivity and Focus Monitor programs

Table 11: Monitored settings: number of lines (first-order CCD)

Grating	Wave	7a	7b	8a	8b	9	10	11	17	18	19	20	21	22	23	24	25
G230LB	2375	35	37	35	35	34	28	37	33	29	31	33	30	30	34	32	23
G230MB	1854							22	21								
	1995	33	37	43	39	40	41	28	19	14	20	23	15	16	16	14	21
	2135							11	8								
	2276							26	21								
	2416	24	34	36	37	32	34	16	19	17	14	16	12	13	14	13	15
	2557							34	25								
	2697	42	49	45	50	47	46	27	21	24	22	16	21	21	19	17	20
	2794							40	40								
	2836							33	35								
	2976							29	28								
	3115	39	44	47	43	44	43	36	33	35	30	33	32	35	26	31	30
G430L	4300	22	22	21	19	21	21	24	26	27	25	25	27	27	28	27	24
G430M	3165	44	45	46	50	47	44	34	34	37	36	39	37	36	36	32	32
	3423							38	41								
	3680	48	46	45	44	45	43	33	32	30	30	33	32	29	31	28	32
	3843							37	31								
	3936							31	26								
	4194	38	42	38	38	39	38	25	27								
	4451							29	36								
	4706							29	32								
	4961	32	33	34	35	34	33	25	23	19	20	25	23	21	20	18	18
	5093							21	21								
	5216							31	30								
	5471	23	25	23	22	24	26	16	13	16	11	17	16	17	15	16	13
G750L	7751	38	38	39	37	37	39	42	46	42	44	42	45	41	42	42	44
	8975	25	25	26	29	26	27										
G750M	5734	22	24	25	23	24	23	23	23	22	23	21	22	22	22	21	23
	6252							24	24								
	6581	16	16	18	17	15	15	13	13								
	6768	10	12	13	11	12	10	9	9	9	10	9	9	9	9	10	9
	7283							13	12								
	7795							7	7								
	8311	17	17	17	17	17	17	17	17	18	17	17	17	16	16	17	17
	8561	23	21	21	22	22	22	20	20								
	8825							21	22								
	9336	28	27	29	26	25	28	17	16	18	17	16	15	15	17	16	16
	9851							9	9								
	10363	7	8	8	8	8	7										

Notes: Lamp for all CCD settings switched from LINE to HITM1 in cycle 11.
Multiple exposures obtained for G230MB/1995 and G230MB/2416 in cycle 25.

Table 12: Current analysis vs. Pas11 and Son15 (first-order MAMA and CCD)

Grating	Wave	$t_{exp}(25)$	Pascucci et al. 2011			Cycle 17			Sonnentrucker 2015			Cycles 19–21		
			offset	stdev	N	offset	stdev	N	offset	stdev	N	offset	stdev	N
G140L	1425	70	-0.05	0.20	41	-0.08	0.22	33	0.03	0.15		0.09	0.23	13
G140M	1218	600	-0.10	0.25	16	0.06	0.21	13	0.03	0.23	8	-0.03	0.23	11
	1222		-0.07	0.46	18	0.16	0.27	10						
	1321		-0.03	0.37	20	0.02	0.29	22						
	1420		-0.01	0.26	19	0.03	0.21	26						
	1540		0.06	0.25	12	0.10	0.24	24						
	1640	150	0.08	0.23	9	0.24	0.19	7			4	0.18	0.24	8
G230L	2376	48	0.01	0.15		0.00	0.21	23	-0.01	0.12		0.04	0.22	26
G230M	1687	310	-0.03	0.20	19	0.08	0.21	18	-0.06	0.34	8	0.01	0.21	22
	2338		-0.10	0.22	7	-0.09	0.21	16						
	2818		-0.11	0.14	8	-0.23	0.14	7						
	3055	22	-0.18	0.12	6	-0.21	0.22	10	-0.24	0.17	4	-0.22	0.20	13
G230LB	2375	240	0.06	0.24		0.05	0.17	33	-0.01	0.29		0.11	0.22	31
G230MB	1854		0.05	0.25	15	0.07	0.22	21						
	1995	3x240	-0.02	0.23	14	0.02	0.25	19	-0.03	0.20	12	-0.01	0.21	19
	2135		-0.12	0.08	5	-0.07	0.19	8						
	2276		0.01	0.22	17	0.01	0.22	21						
	2416	2x50	0.11	0.12	8	0.19	0.14	19	0.03	0.22	6	0.09	0.25	14
	2557		-0.01	0.33	16	-0.12	0.17	25						
	2697	20				0.07	0.22	21	0.02	0.27	8	0.05	0.19	20
	2794		0.04	0.24	21	0.09	0.20	40						
	2836		0.02	0.25	27	0.09	0.22	35						
	2976		0.12	0.16	20	0.26	0.13	28						
	3115	27	0.05	0.20	22	0.17	0.17	33	-0.04	0.20	18	0.11	0.18	32
G430L	4300	11	-0.02	0.28		-0.16	0.22	26	-0.01	0.27		-0.08	0.21	26
G430M	3165	11	0.16	0.23	12	0.04	0.16	34	0.04	0.16	8	0.03	0.16	37
	3423		0.00	0.26	6	0.11	0.11	41						
	3680	11	0.12	0.18	8	0.15	0.18	32	0.00	0.29	7	0.17	0.20	32
	3843					0.07	0.16	31						
	3936		0.13	0.43	3	0.06	0.13	26						
	4194		0.02	0.13	4	-0.17	0.15	27						
	4451		0.06	0.19	23	0.08	0.19	36						
	4706		0.15	0.28	21	0.13	0.21	32						
	4961	24	-0.05	0.07	10	-0.02	0.14	23	-0.07	0.11	11	0.02	0.14	23
	5093		0.06	0.11	8	0.05	0.18	21						
	5216		-0.02	0.07	14	0.03	0.17	30						
	5471	26	0.06	0.12	11	0.15	0.09	13	0.07	0.09	9	0.16	0.11	15
G750L	7751	6.2	-0.07	0.15		-0.12	0.11	46	-0.08	0.17		-0.08	0.11	44
	8975													
G750M	5734	5.9	0.01	0.07	16	0.03	0.11	23	-0.01	0.09	14	0.04	0.09	22
	6252		0.09	0.08	17	0.12	0.09	24						
	6581		0.09	0.14	11	0.17	0.07	13						
	6768	3.9	-0.01	0.04	9	0.06	0.03	9	-0.01	0.04	9	0.06	0.03	9
	7283		0.04	0.06	9	0.11	0.04	12						
	7795		0.12	0.12	5	0.17	0.15	7						
	8311	10	0.06	0.09	17	0.12	0.06	17	-0.02	0.06	17	0.05	0.06	17
	8561		0.02	0.07	19	0.10	0.07	20						
	8825		0.04	0.06	17	0.15	0.12	22						
	9336	10	-0.01	0.10	14	0.05	0.09	16	-0.03	0.07	13	0.07	0.13	16
	9851		0.14	0.12	2	0.10	0.08	9						

Notes: $t_{exp}(25)$ is the exposure time used in cycle 25.
G230L/2376 is at a lamp current of 3.8 mA; all others are at 10 mA.
All lines in settings G430L/4300 and G430M/3165–4194 appear to have been misidentified in Pas11 and Son15.